What lurks below the last plateau

15+ years of 0.7: What have we learned and where to next?

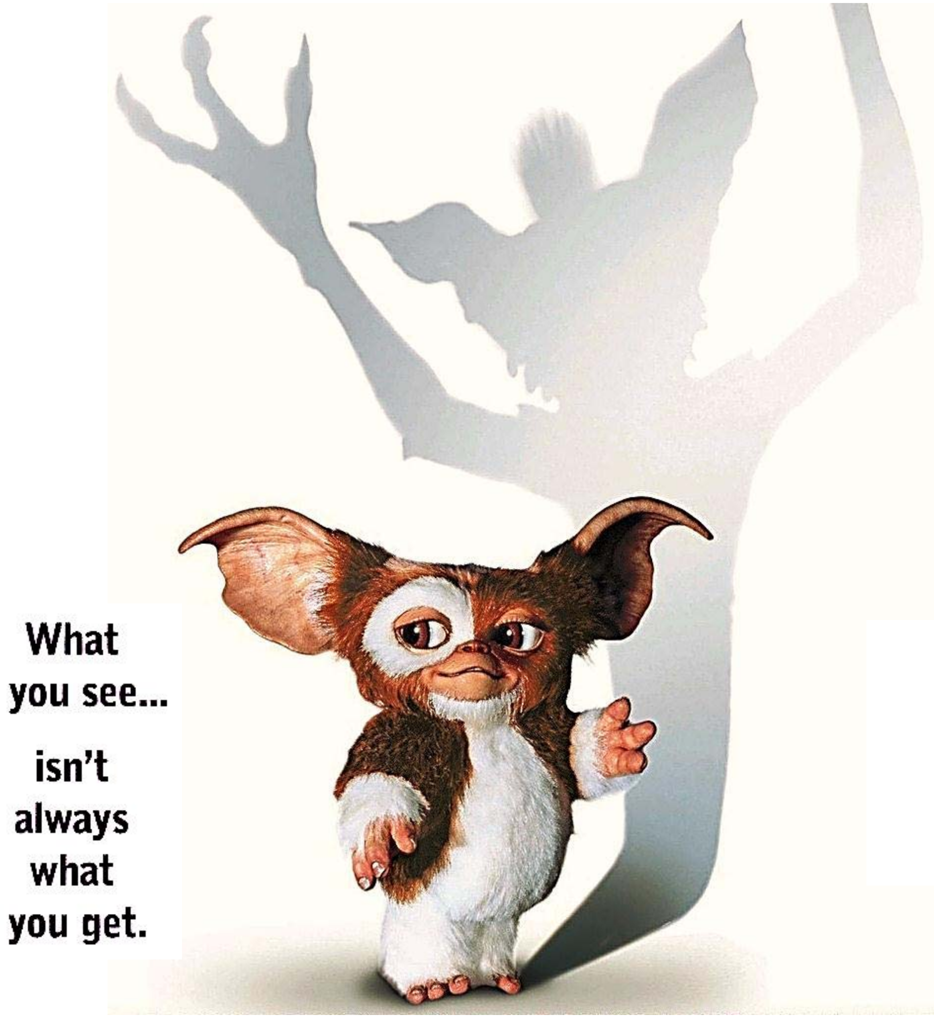

<u>Lecture 2</u>: Spin-gap models and 1D subband behaviour

Adam Micolich

Nanoelectronics Group
School of Physics, UNSW.

Let's start with the differential conductance

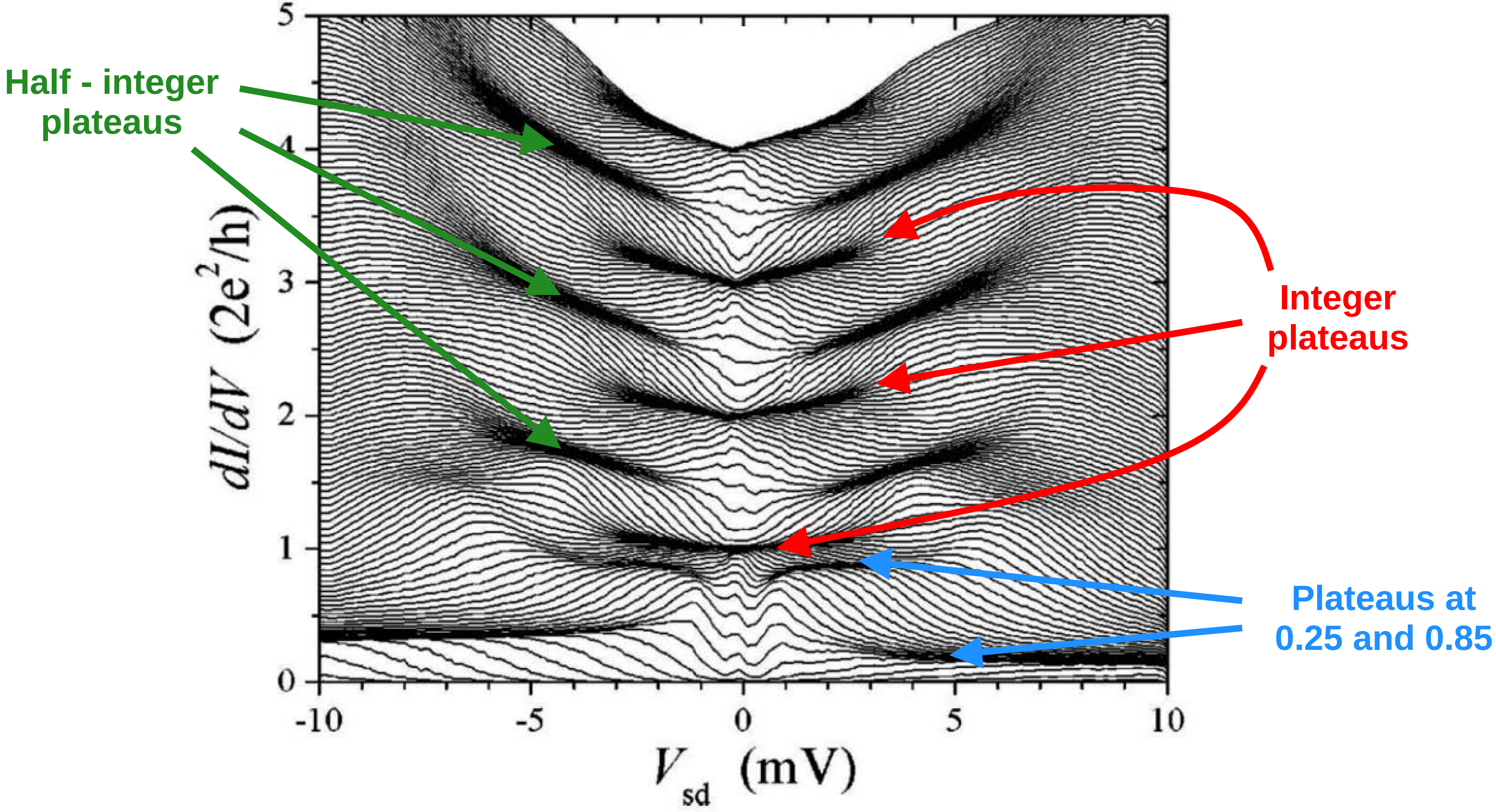

A. Kristensen *et al.*, PRB 62, 10950 (2000).

Let's start with the differential conductance

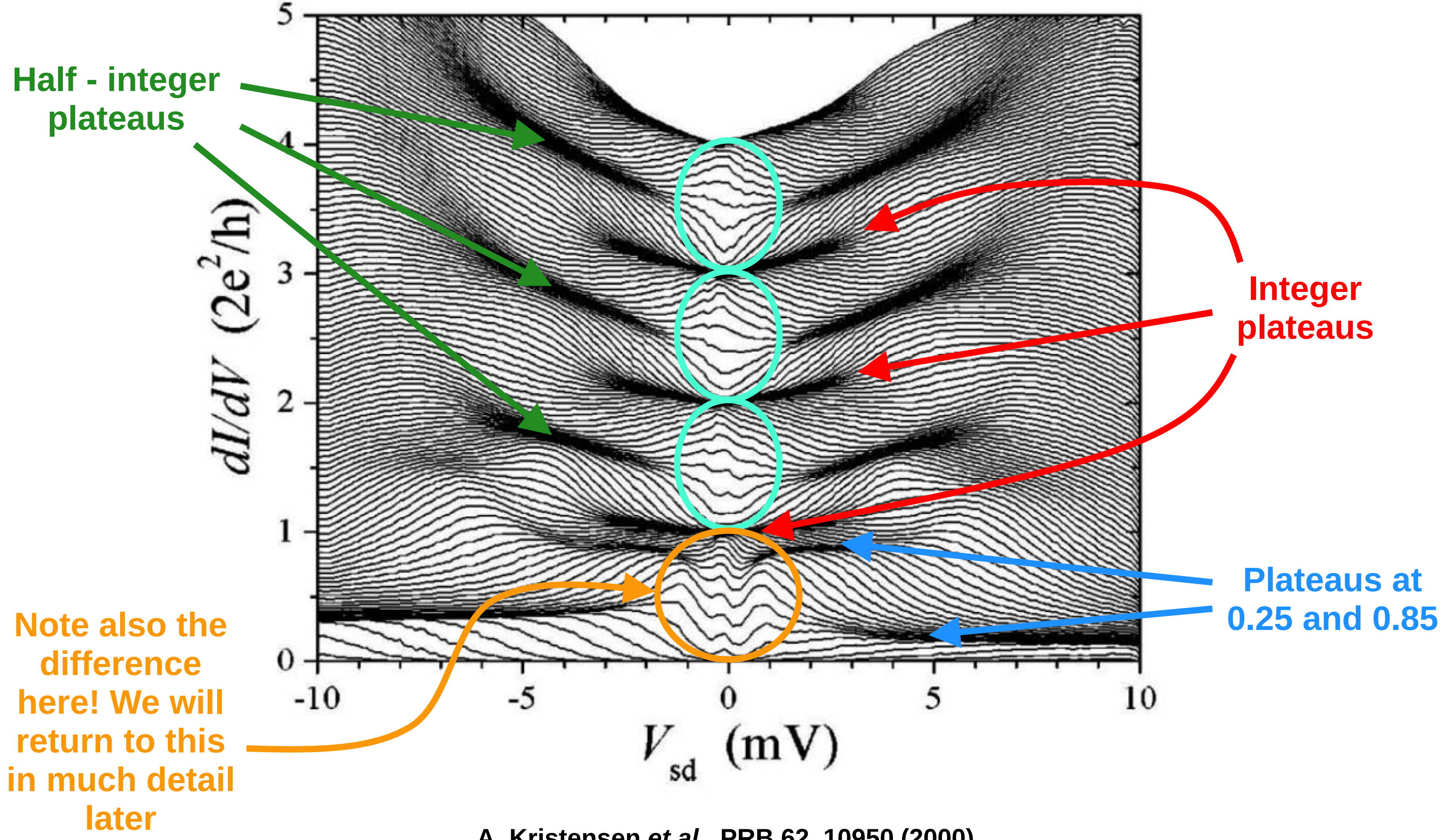

A. Kristensen *et al.*, PRB 62, 10950 (2000).

The transconductance greyscale

0.7 is tucked away in here

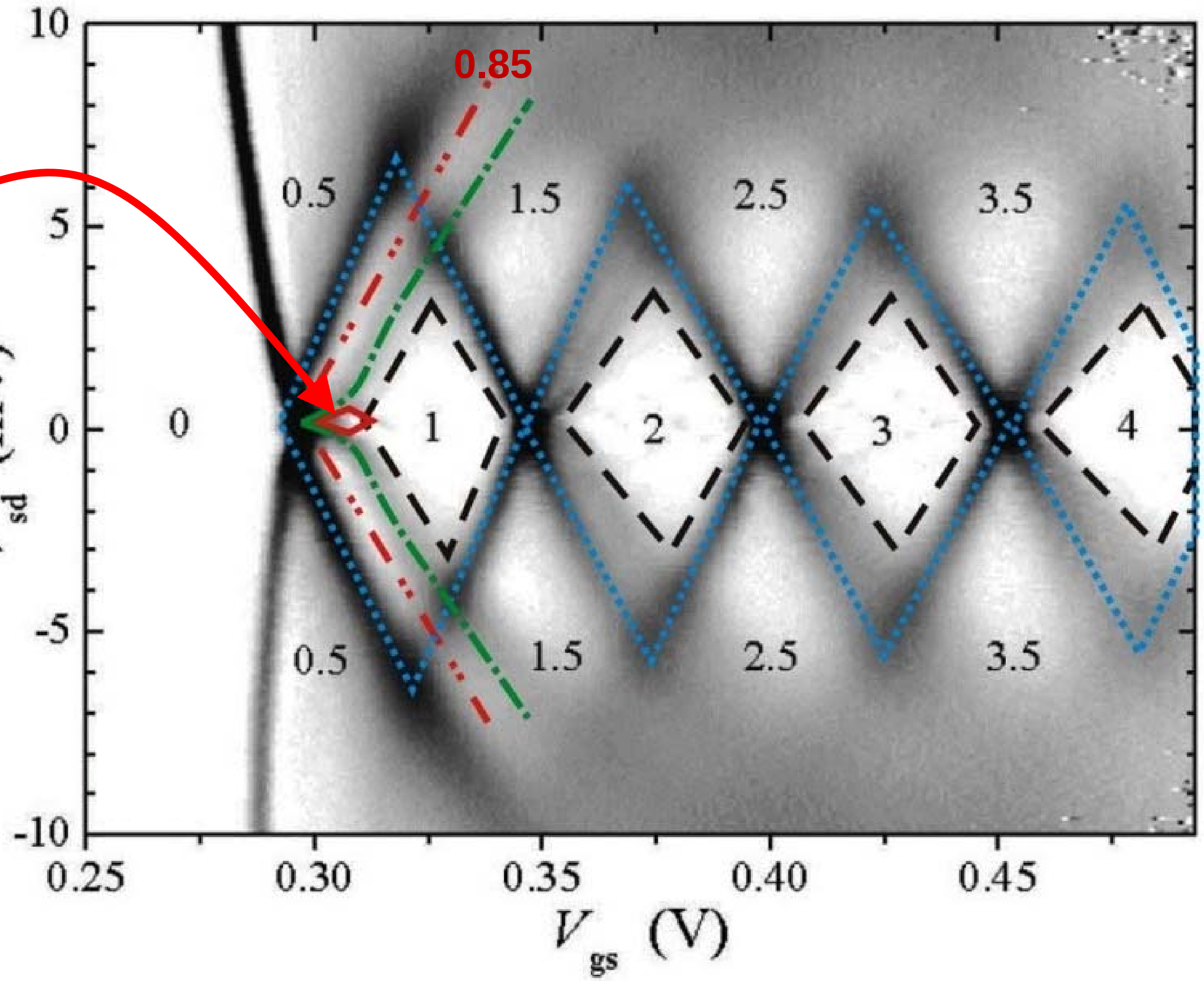

A. Kristensen *et al.*, PRB 62, 10950 (2000).

Taking a closer look…

- **The 1st subband crosses the drain twice !?! But how ?**

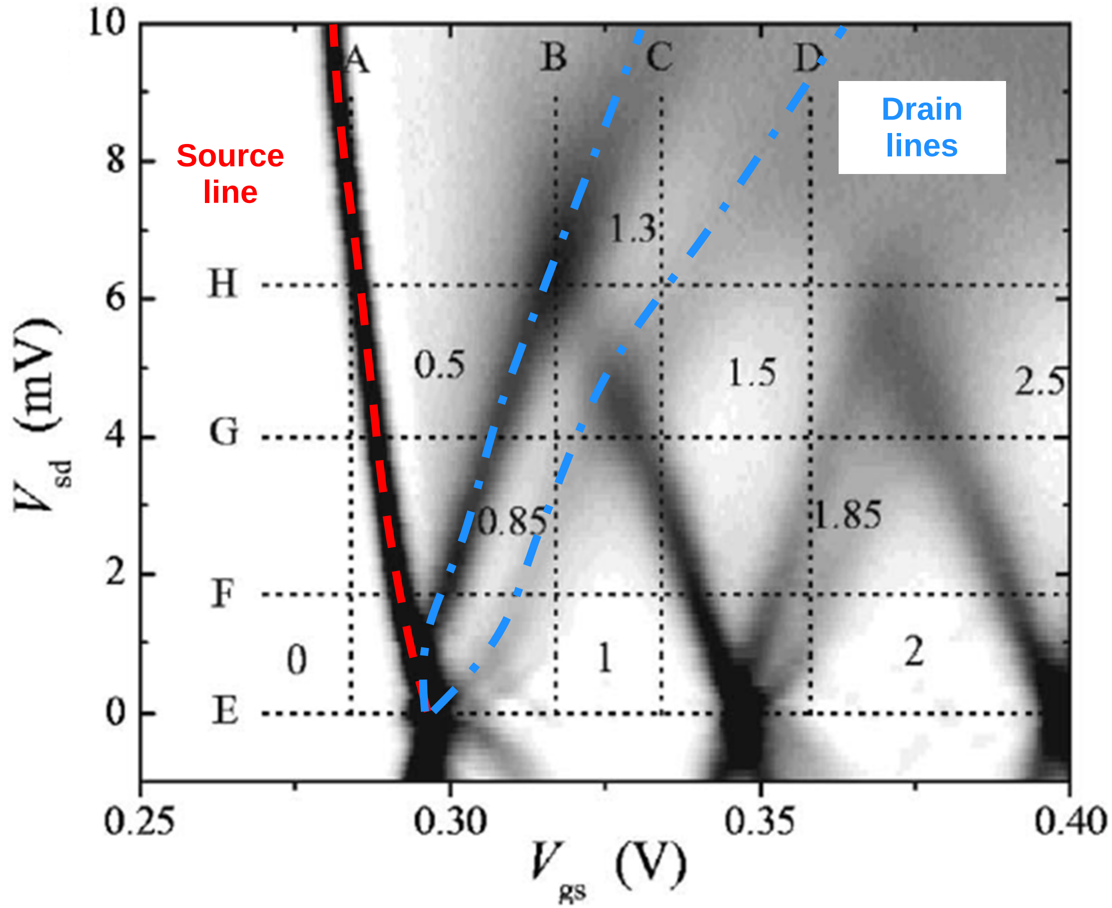

A. Kristensen *et al.*, PRB 62, 10950 (2000).

An anomalous subband edge

- **Associate 0.7 plateau with an anomalous subband edge ε_0' split off from and laying above the ordinary edge ε_0.**
- **ε_n' splits off from ε_n only for $\mu = (\mu_s + \mu_d)/2 > \varepsilon_n$ (i.e., once subband drops below E_F).**

This arm is ε_0 and ε_0 prior to split-off.

This arm is caused by ε_0

This arm is caused by ε_0'

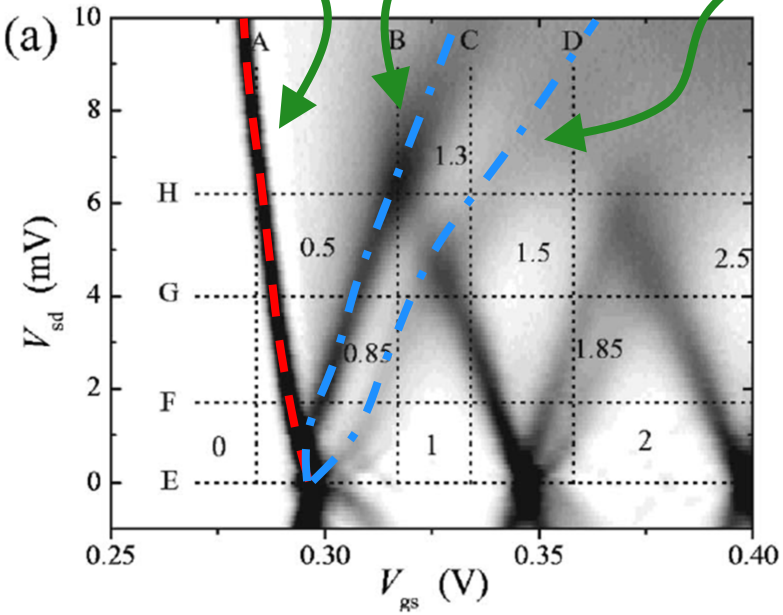

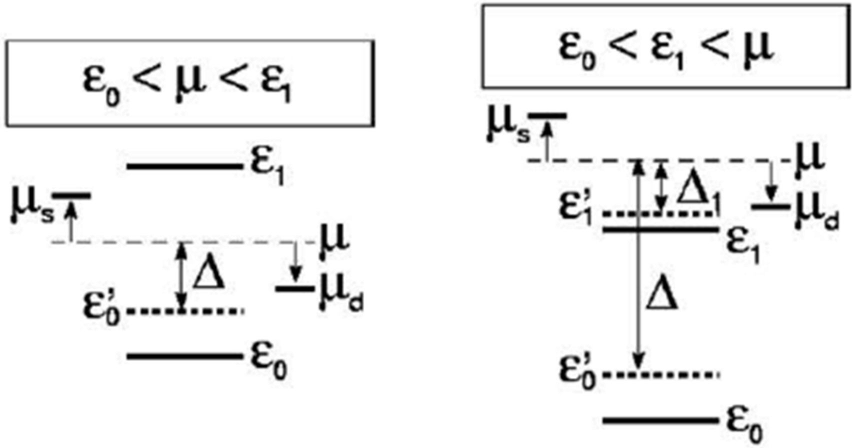

A. Kristensen *et al.*, PRB 62, 10950 (2000).

The Bruus, Cheianov & Flensberg (BCF) Model

- **Here the 'normal' and 'anomalous' subband edges in Kristensen *et al*. are the spin-up and spin-down branches of the 1D subband.**

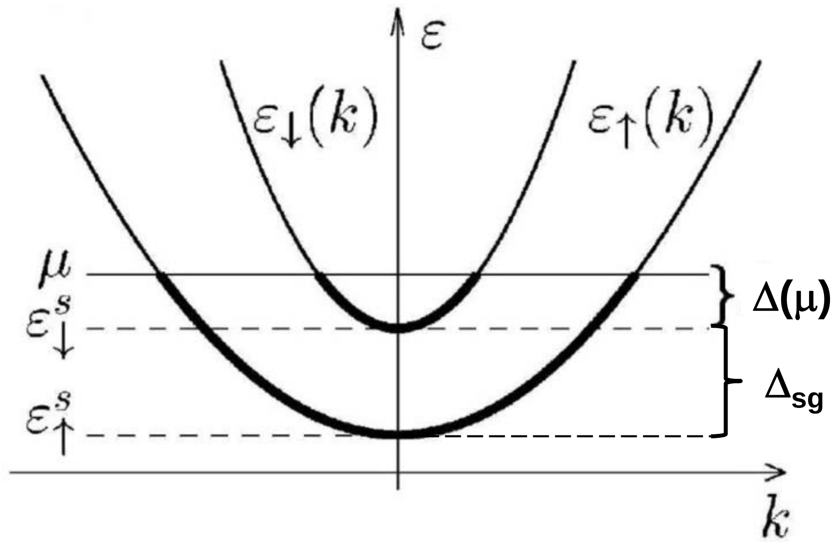

Caution: BCF uses the *opposite* spin convention to all other papers on 0.7. Here spin-up is the lowest level.

- **These contribute to a temperature-dependent conductance:**

$$G(T) = \tfrac{1}{2}(f[\epsilon_\uparrow^S(\mu) - \mu] + f[\epsilon_\downarrow^S(\mu) - \mu])G_0$$

where $f[x] = (\exp(x/k_B T) + 1)^{-1}$ is the Fermi-Dirac distribution, and $\mu = (\mu_s + \mu_d)/2$.

H. Bruus *et al.,* Physica E 10, 97 (2001) and arXiv:Cond-mat/0106504.

The Bruus, Cheianov & Flensberg (BCF) Model

- **The important energy scale in this model is the Fermi energy of the spin-down subband $\Delta(\mu) = \mu - \varepsilon^{s}_{\downarrow}(\mu)$, relative to the spin-gap energy Δ_{sg} and $k_B T$.**

$\Delta(\mu) >> \Delta_{sg}$: The spin-polarization is weak and there is a single plateau at $2e^2/h$ ($= G_0$).

$\Delta(\mu) < \Delta_{sg}$: Stronger spin-polarization and the conductance near the low G edge of the $2e^2/h$ plateau becomes temperature dependent.

if this holds, *and*:

$k_B T << \Delta(\mu), \Delta_{sg}$: both $f[x] = 1$, giving $G = G_0 \Rightarrow$ there is no 0.7 plateau.

$\Delta(\mu) < k_B T < \Delta_{sg}$: the first $f[x]$ falls to 0.5, giving $G = 0.75\ G_0 \Rightarrow$ ~0.7 plateau.

$\Delta(\mu), \Delta_{sg} << k_B T$: both $f[x]$ fall to 0.5, giving $G = 0.5\ G_0 \Rightarrow$ second plateau at ~0.5.

In the second instance, for finite V_{sd}, the conductance falls by 1/8 G_0 giving a finite bias plateau at 0.875 G_0 (but also at 0.75 G_0 at higher T).

H. Bruus *et al.*, Physica E 10, 97 (2001) and arXiv:Cond-mat/0106504.

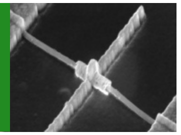

The Bruus, Cheianov & Flensberg (BCF) Model

- **Sometimes this model gives behaviour that looks very promising…**

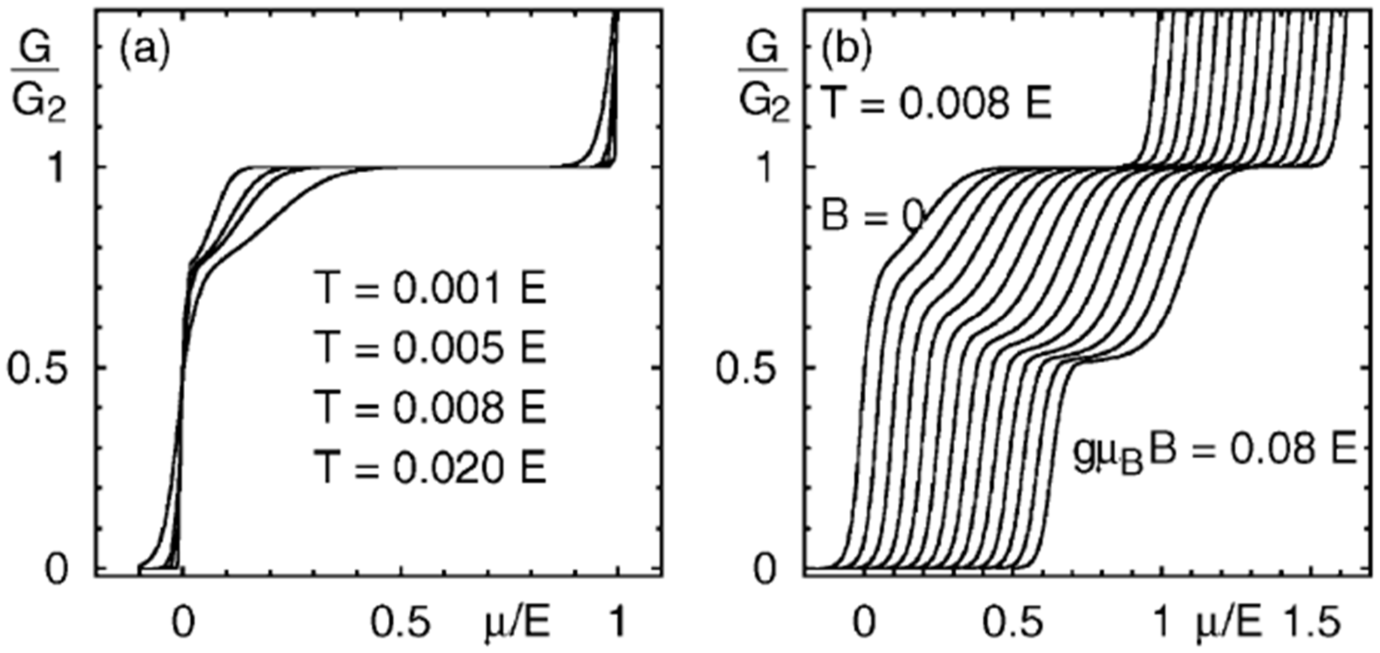

H. Bruus *et al.*, Physica E 10, 97 (2001) and arXiv:Cond-mat/0106504.

The Bruus, Cheianov & Flensberg (BCF) Model

- **Sometimes this model gives behaviour that looks very promising…**

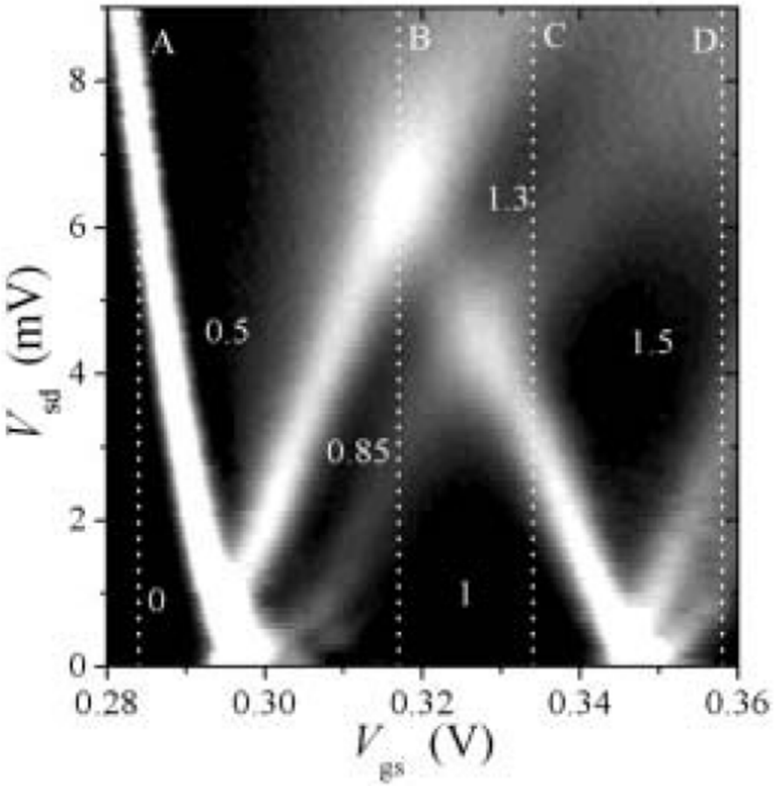

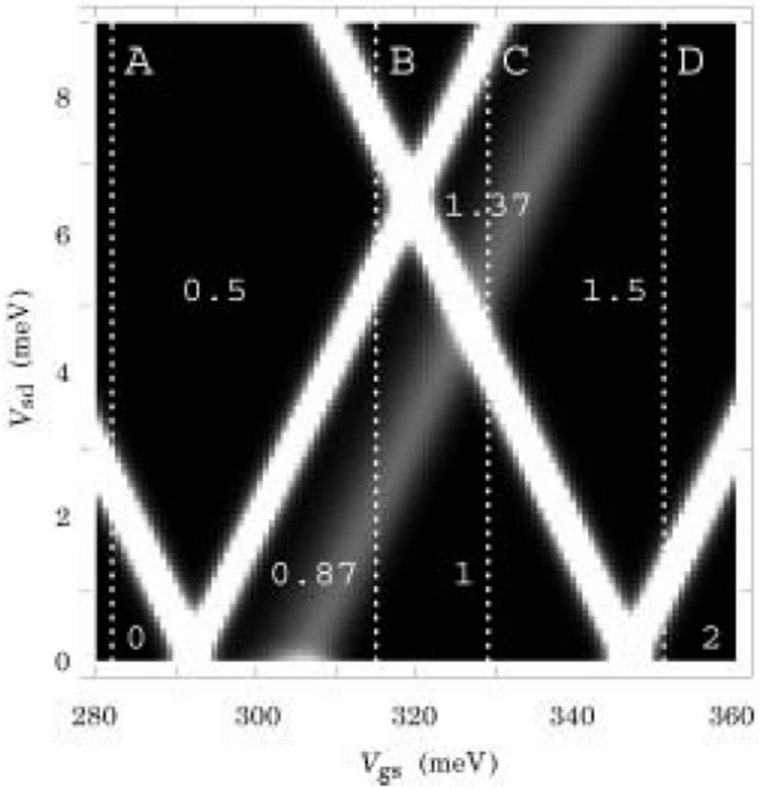

A. Kristensen & H. Bruus, Physica Scripta T101, 151 (2002).

The Bruus, Cheianov & Flensberg (BCF) Model

… and sometimes it doesn't.

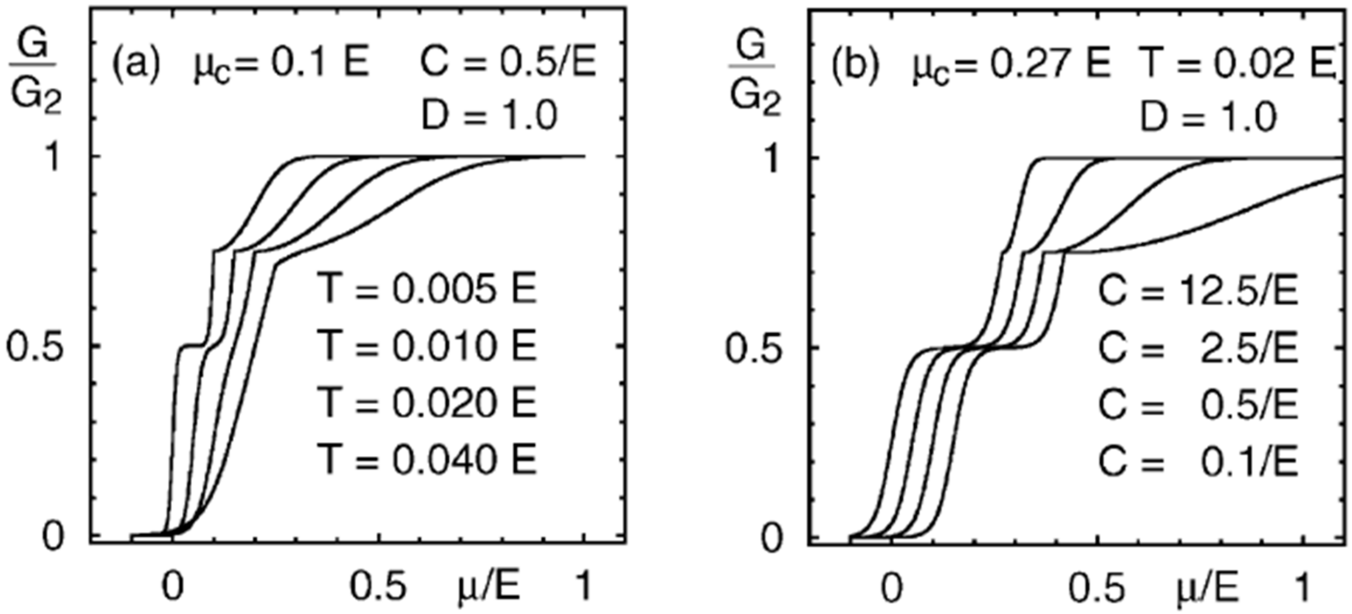

- **The tendency for two plateaus is probably the biggest flaw in this phenomenological model. It is something that isn't observed experimentally.**

H. Bruus *et al.*, Physica E 10, 97 (2001) and arXiv:Cond-mat/0106504.

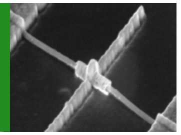

But is there really activation?

0.7 as a thermal activation effect

- **Kristensen *et al*. looked at the temperature dependence of the conductance at the low G edge of the G_0 plateau.**
- **If there is activated behaviour, the conductance here should behave like $G(T)/G_0 = 1 - C \exp(-T_A/T)$.**

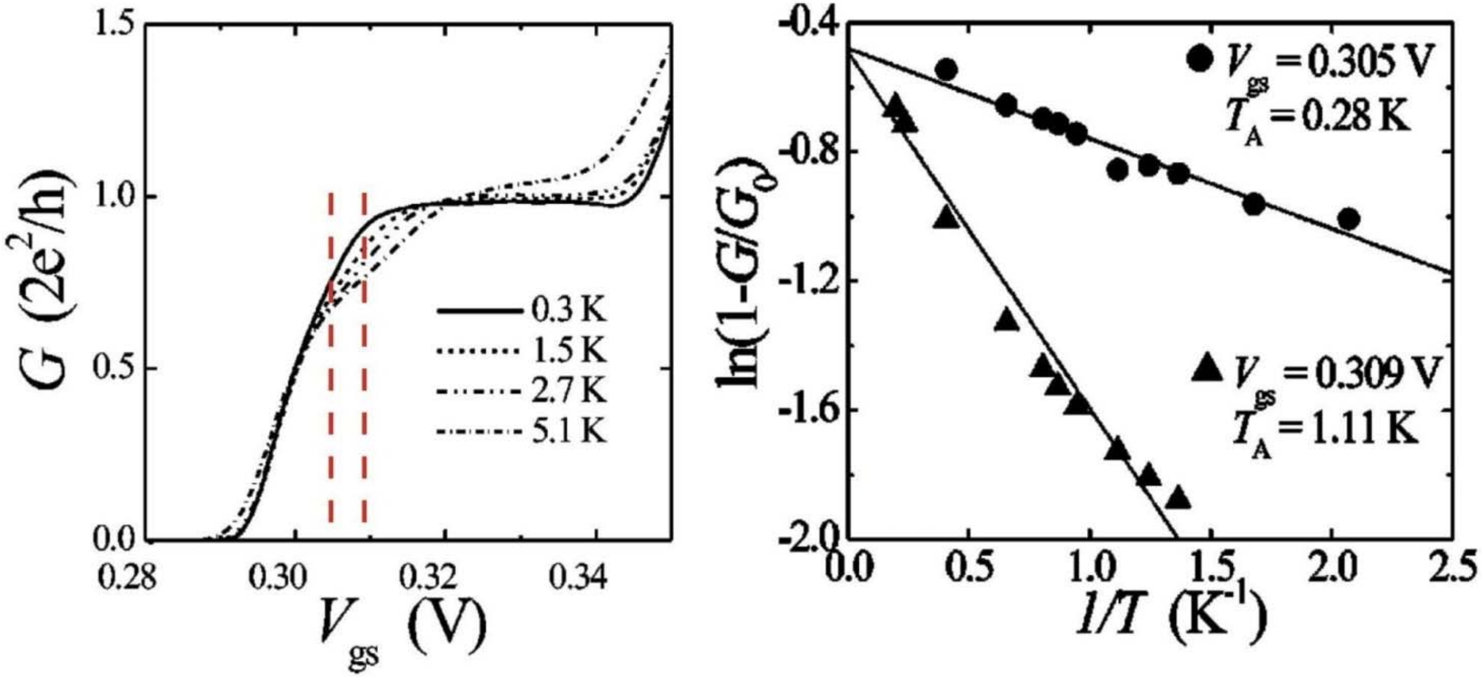

A. Kristensen *et al.,* PRB 62, 10950 (2000).

0.7 as a thermal activation effect

- Repeating this analysis gives a rising T_A with V_{gs}. Converting T_A into an equivalent source-drain bias using $V_{sd}^*=2k_BT_A/e$ and plotting against V_{gs} in the transconductance greyscale reveals something very interesting.

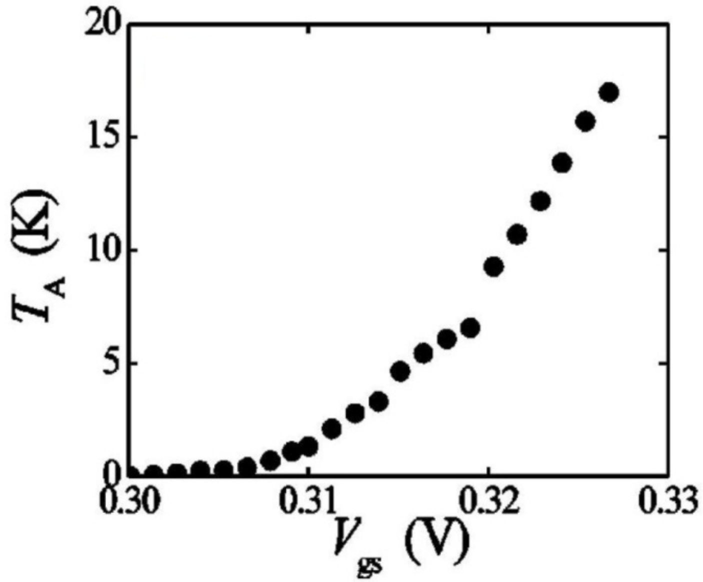

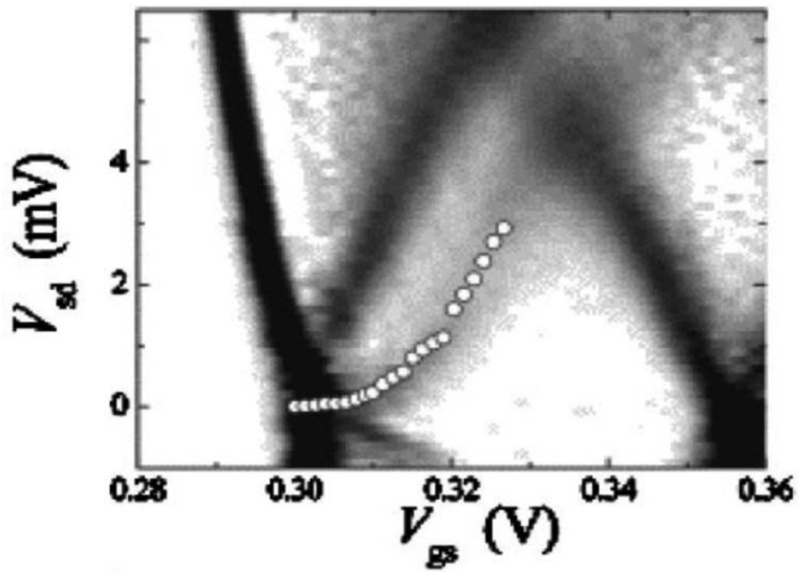

- Strong evidence that there is thermal activation involved in 0.7.

A. Kristensen *et al.,* PRB 62, 10950 (2000).

To show it's not an isolated case…

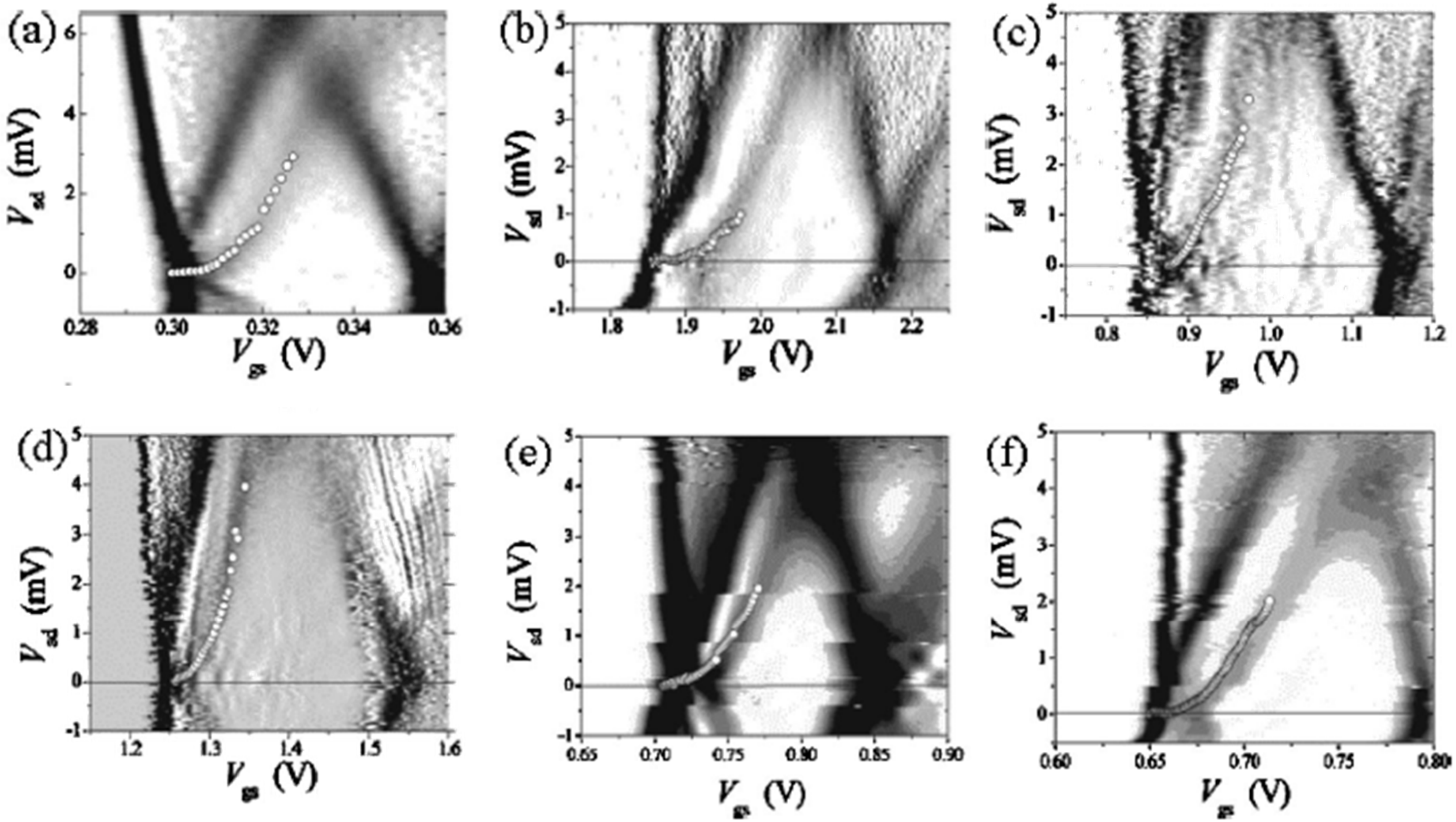

A. Kristensen *et al.,* PRB 62, 10950 (2000).

Back to BCF for a moment

- **How exactly does the gap open in the BCF model?**

Δ_{sg} must be zero until after the subband edge passes μ_s, as there is only one left-moving branch in the transconductance greyscale.

In the BCF model, the gap doesn't open until the subband edge reaches μ_d.

However, providing the relationship to other energy scales is correctly accounted for, it can potentially be finite but small after the subband edge passes μ_s without adversely affecting the model.

Looking at the exact form used…

A. Kristensen & H. Bruus, Physica Scripta <u>T101</u>, 151 (2002).

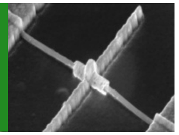

Back to BCF for a moment

- **The form mentioned in the paper is $\varepsilon'_0(\mu_d) = \mu_d(1 - (\mu_d/\mu^*)^n)$ with $0 < \mu_d < \mu^*$ where $\mu^* = 4$ meV and $n = 3$, but what's plotted is $\varepsilon'_0(\mu_d) = \mu_d(1 - (\mu_d/\mu^*))^n$.**

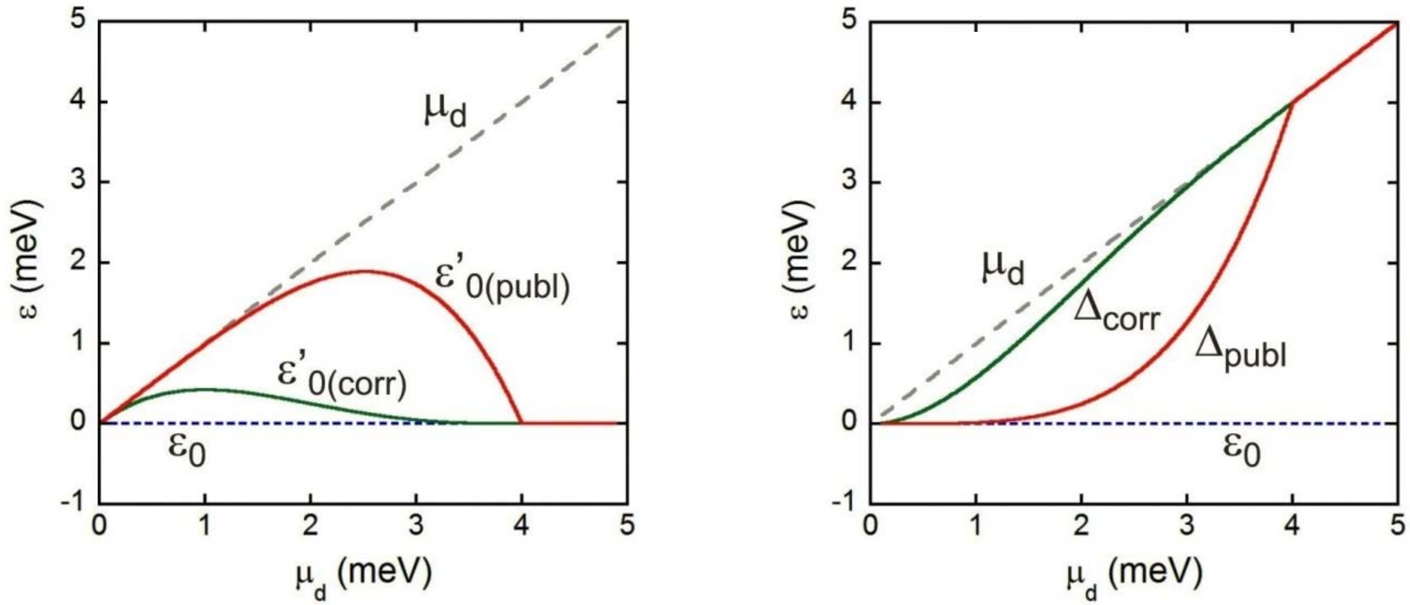

- **The values for μ^* and *n*, and the form, are chosen based on an empirical analysis of the experimental data, but the essential point is that the gap must not open before the 1D subband edge passes μ_s.**

A. Kristensen & H. Bruus, Physica Scripta T101, 151 (2002).

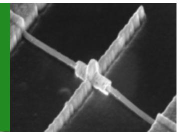

The density-dependent spin-gap model

The gap opens linearly with increasing gate voltage/density

Eventually, the rising Fermi energy catches the spin-up subband

Here the gap opens as soon as the subband populates (i.e., reaches μ_s)

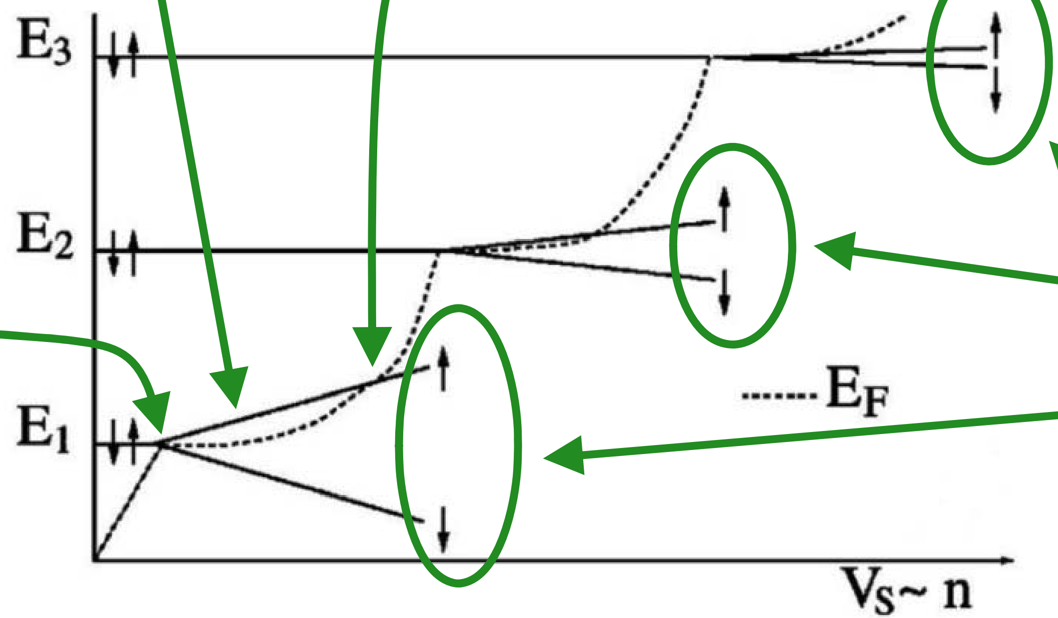

One free parameter – the opening rate with V_g or n

D.J. Reilly *et al.*, PRL 89, 246801 (2002).

The density-dependent spin-gap model

- **From the Fermi energy's perspective it looks like…**

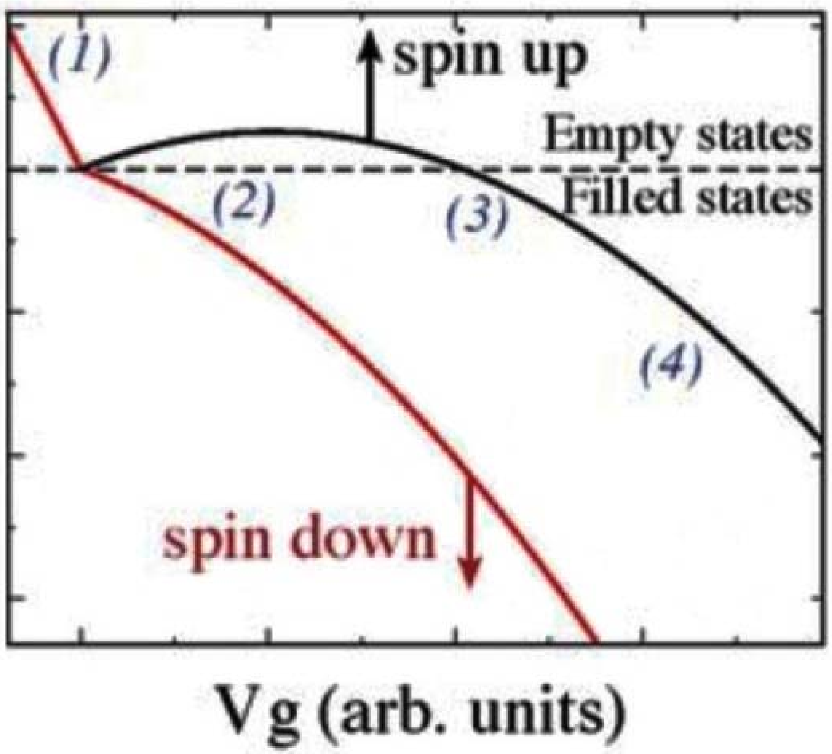

This is clearly another case where thermal activation is vital to the model.

D.J. Reilly *et al.*, Physica E 34, 27 (2006).

The density-dependent spin-gap model

- Formally, the conductance is calculated using:

$$G = 2e^2/\mathrm{h}\int_{U_L}^{\infty}(-\partial f/\partial E)T(E)dE$$

where U_L is the bottom of the band in the left lead, f is the Fermi function f = [1/exp(($E_{\uparrow\downarrow}$ – E_F)/k_BT) + 1] and $E_{\uparrow\downarrow}$ are separately the spin-up/down subband edges.

A classical step function is used for the transmission probability $T(E) = \Theta(E_F - E_{\uparrow\downarrow})$ where $\Theta(x) = 1$ for $x > E_{\uparrow\downarrow}$ and $\Theta(x) = 0$ for $x < E_{\uparrow\downarrow}$.

- Hence, the linear response conductance of each spin-band is the Fermi probability for thermal occupation multiplied by the spin-polarized conductance quantum:

$$G \sim e^2/h\, f\uparrow + e^2/h\, f\downarrow$$

D.J. Reilly *et al.*, PRB 72, 033309 (2005).

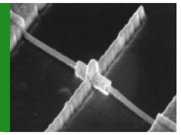

The density-dependent spin-gap model

- **A key advantage is that the opening gap removes the 0.5 plateau in the BCF model.**

$\Delta E_{\uparrow\downarrow}$ opens slowly such that the Fermi function also overlaps $E_{\uparrow}$ giving a 0.7 at even at low T.

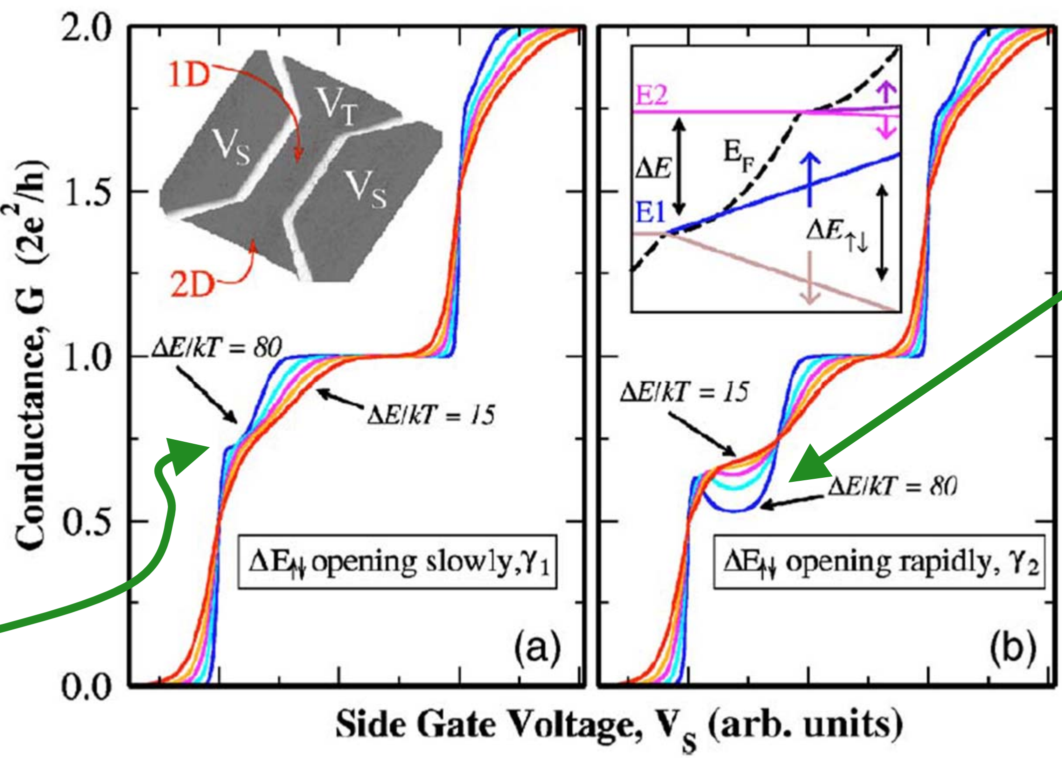

$\Delta E_{\uparrow\downarrow}$ opens rapidly so that $E_{\uparrow}$ escapes the Fermi function briefly to give a dip in towards 0.5. This turns up in real data.

D.J. Reilly *et al.*, PRB 72, 033309 (2005).

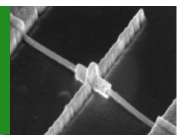

The density-dependent spin-gap model

- **In the Reilly model, the opening rate γ is linked to the 1D-2D mismatch, based on the data below, which can be modelled by changing γ at fixed *T*.**

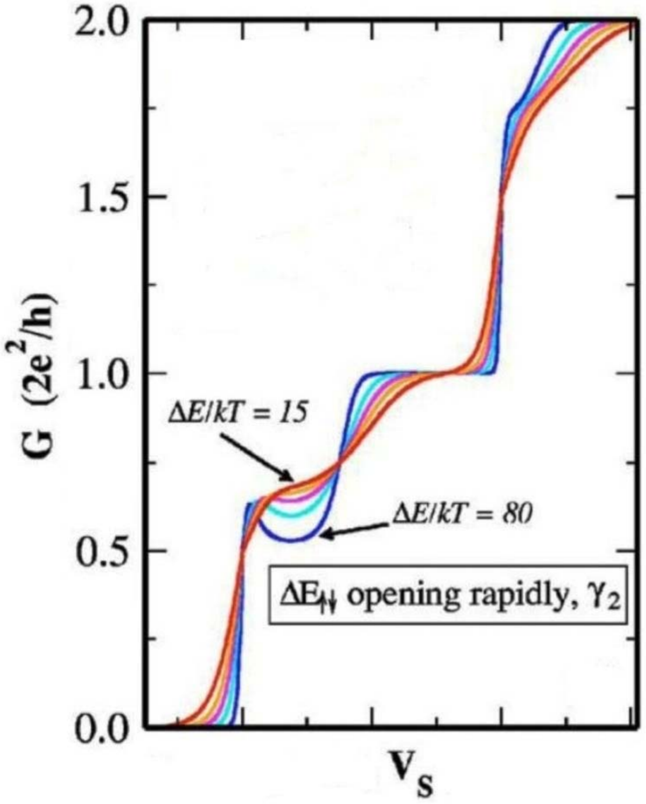

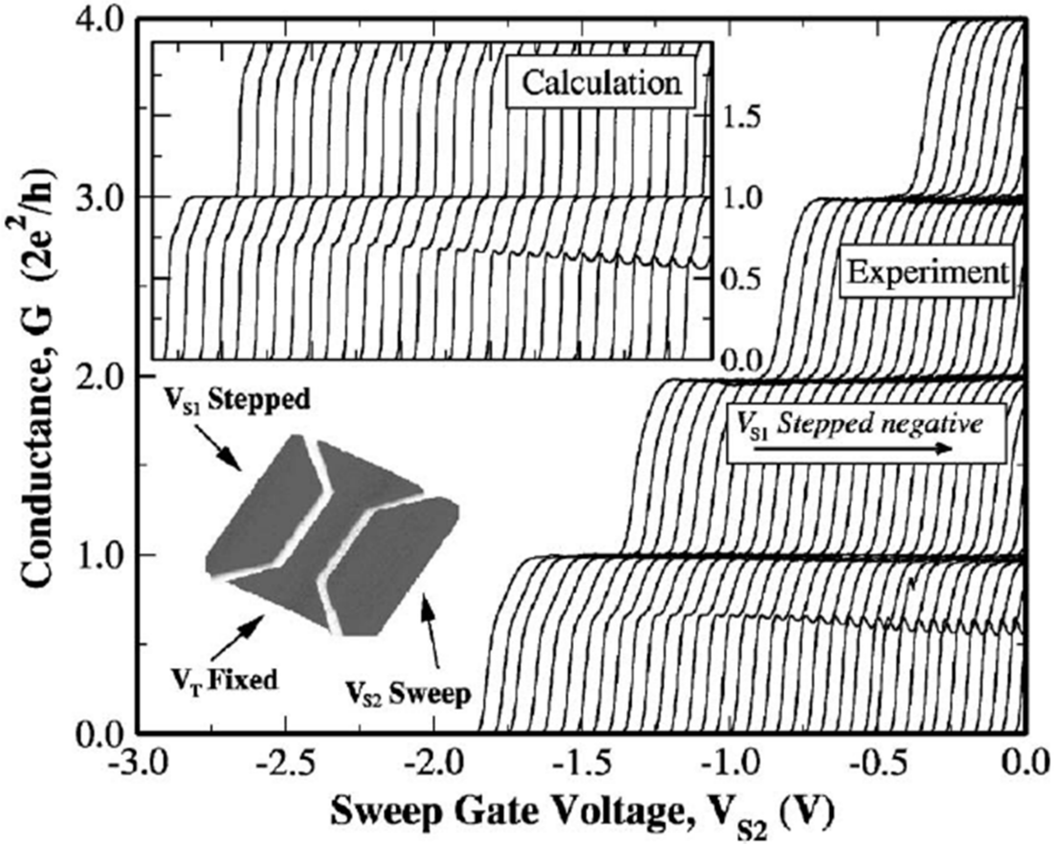

D.J. Reilly *et al.*, PRB 72, 033309 (2005).

The density-dependent spin-gap model

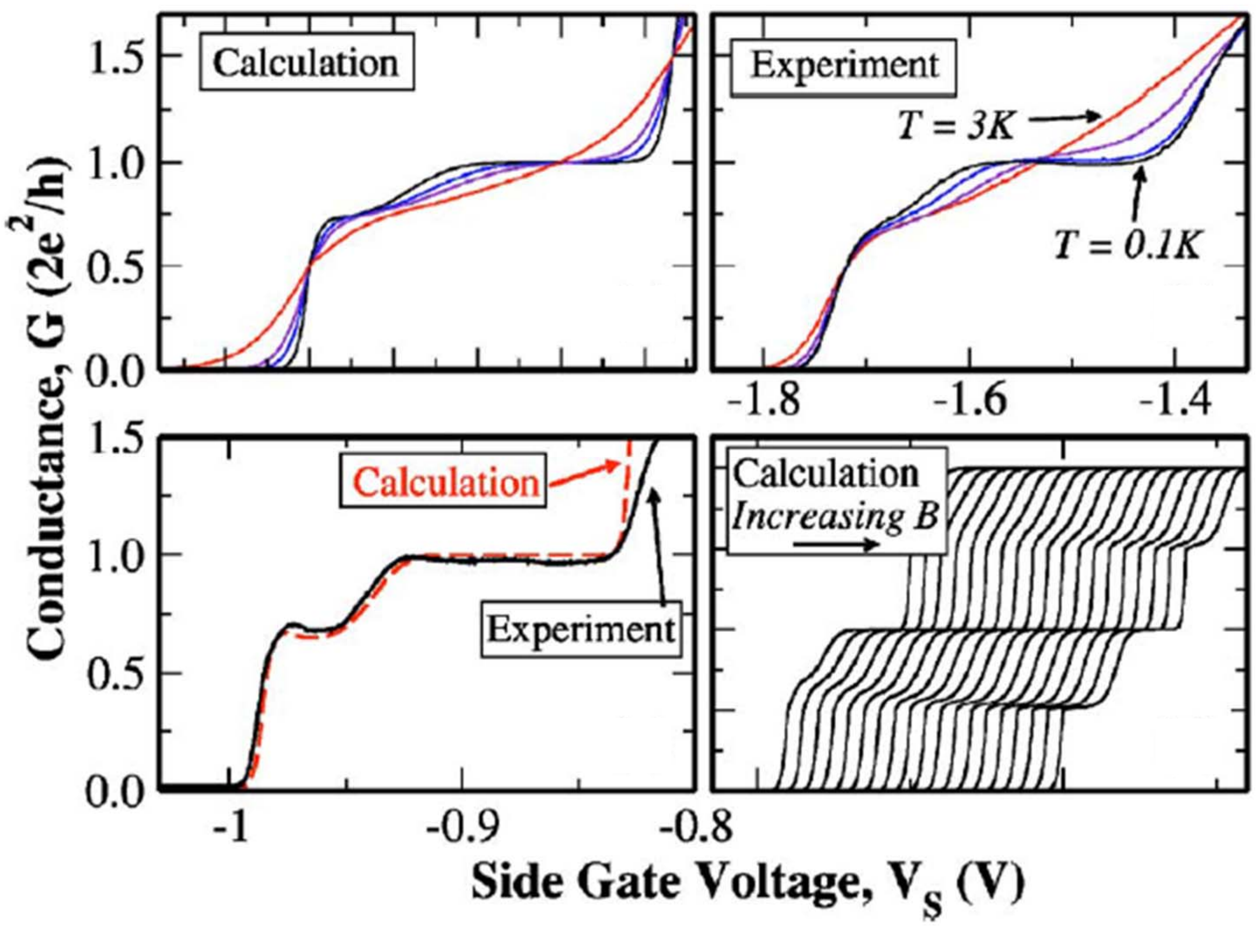

D.J. Reilly *et al.*, PRB 72, 033309 (2005).

The density-dependent spin-gap model

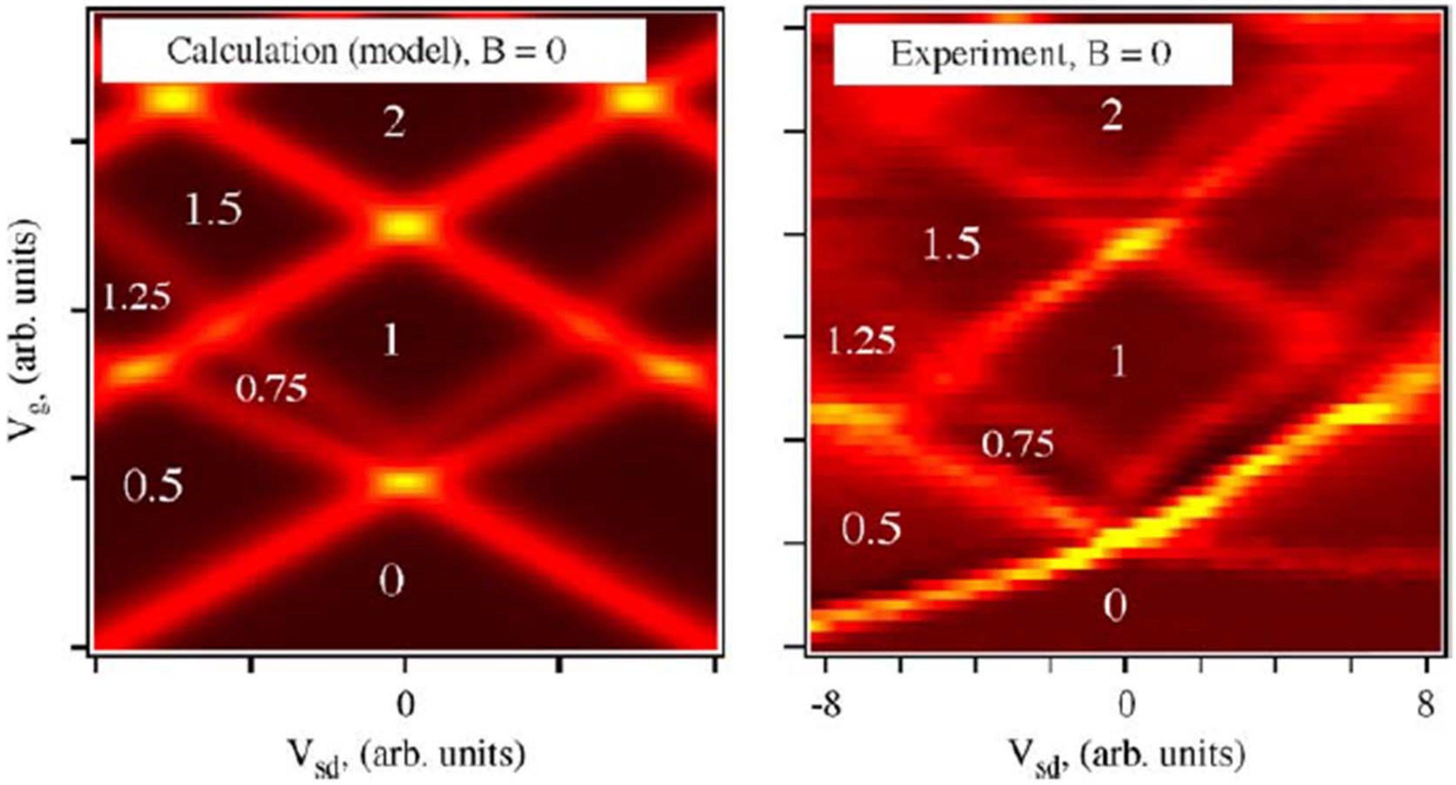

D.J. Reilly *et al.*, Physica E <u>34</u>, 27 (2006).

Quick primer on shot noise

- Shot noise arises due to the discreteness of charge (i.e., electrons carry 1.6×10^{-19} C).
- In a mesoscopic system there is excess noise beyond thermal noise due to ‘partition’.
- Partition noise comes about due to scattering, which ‘partitions’ electrons into one of two channels – a transmitted channel and a reflected channel.
- The partition noise vanishes in the limits $T = 1$ and $T = 0$ as no partitioning takes place. The partition noise is maximal for $T = ½$.
- The transmitted current noise power is given by:

$$S_{I_T I_T} = 2\frac{e^2}{2\pi\hbar}\int \mathrm{d}E\, Tf(1 - Tf)$$

so that if T is very small or f is small, then $1 - Tf = 1$ and S takes its ‘Poisson’ value of $S_P = 2e\langle I\rangle$. At zero temperature, the partition noise is always between 0 ($T = 1$) and S_P.

Y. Blanter & M. Büttiker, Phys. Rep. 336, 1 (2000).

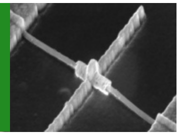

Shot noise and 0.7

- Di Carlo *et al.* measured the partition noise S_I^P of a QPC near the lowest two 1D subbands. This is the total current noise minus the Johnson noise $4k_BTg(V_{sd})$.

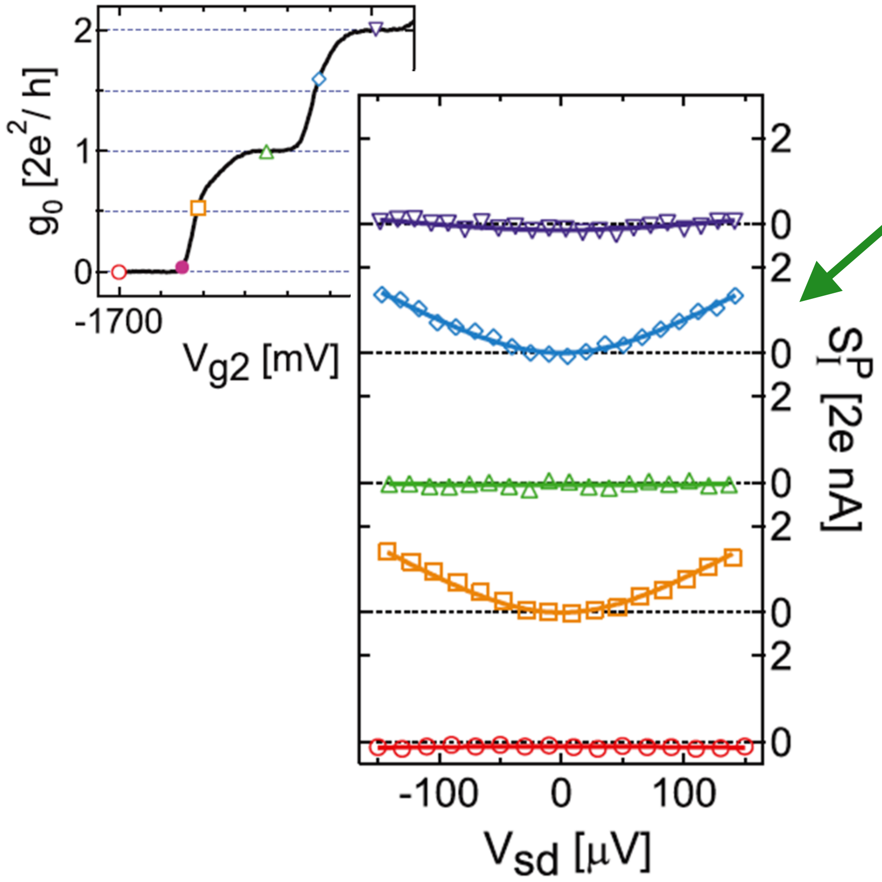

Take $S_I^P(V_{sd})$ data for a whole range of gate voltages V_{g2} and then fit:

$$S_I^P(V_{\rm sd}) = 2\frac{2e^2}{h}\mathcal{N}\left[eV_{\rm sd}\coth\left(\frac{eV_{\rm sd}}{2k_BT_e}\right) - 2k_BT_e\right],$$

to them all, where the noise factor $\aleph$ is the only fit parameter.

For spin-degenerate transmission $\aleph$ vanishes at multiples of G_0 and takes its maximal value of 0.25 at odd multiples of $0.5G_0$.

L. DiCarlo *et al*., PRL 97, 036810 (2006).

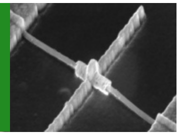

Shot noise and 0.7

- **'Model' here means the density-dependent spin-gap model.**

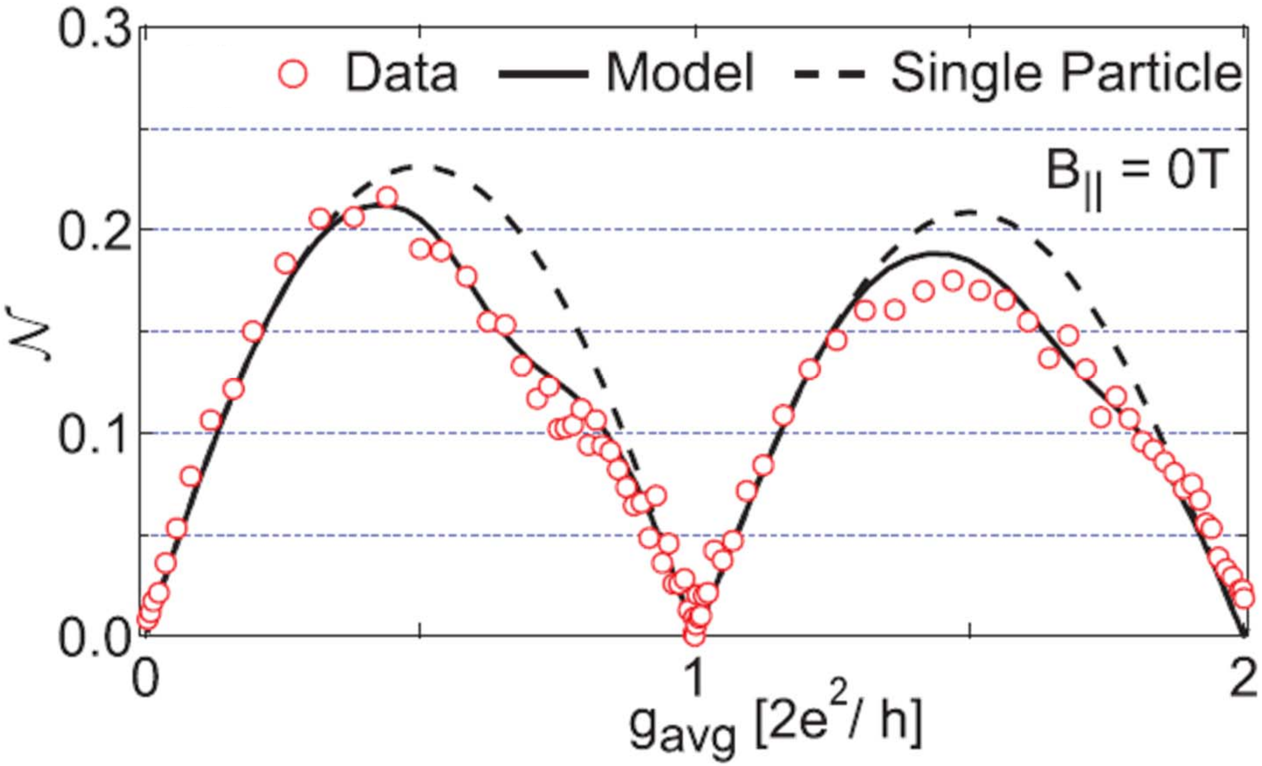

L. DiCarlo *et al*., PRL 97, 036810 (2006).

Shot noise and 0.7

- **Simple Zeeman splitting applied with a 1D enhanced *g*-factor of $g^*_1 = 0.6$.**

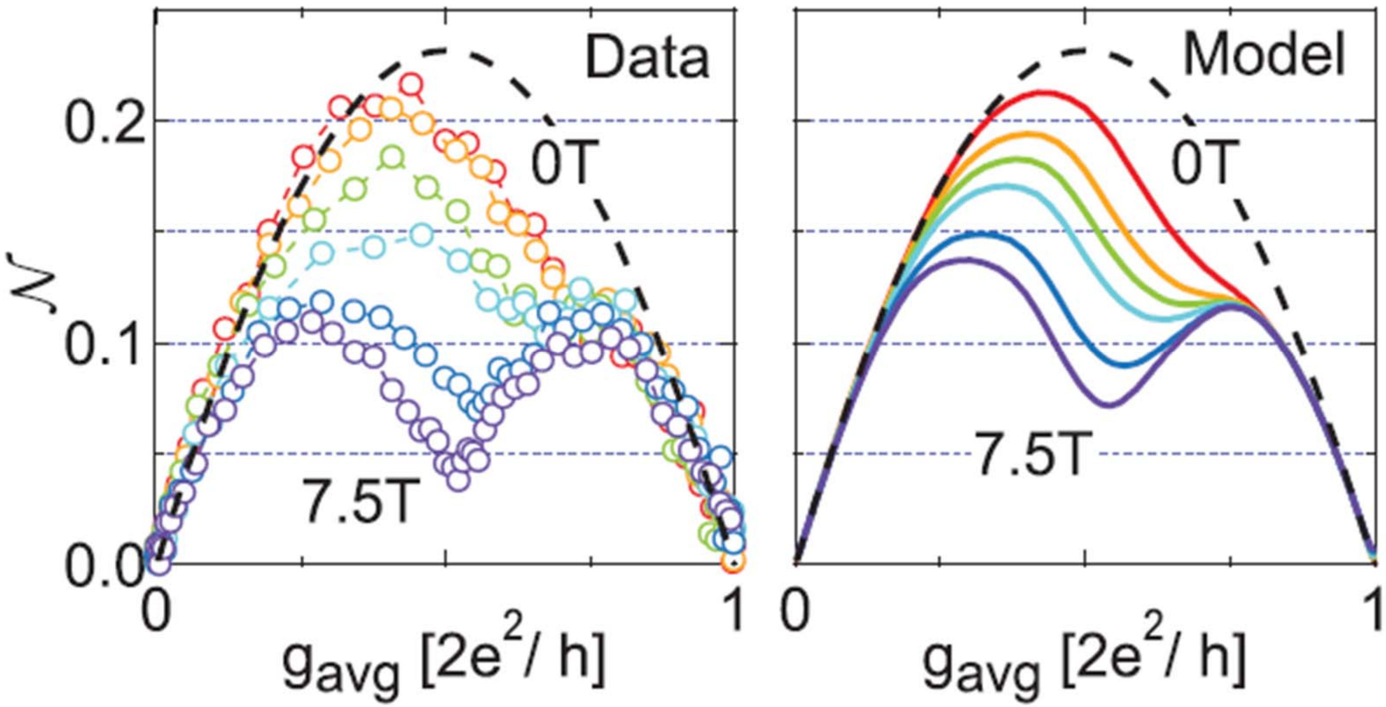

L. DiCarlo *et al*., PRL 97, 036810 (2006).

0.7 with density is a mystery

- **Sometimes the 0.7 plateau rises with increasing density…**

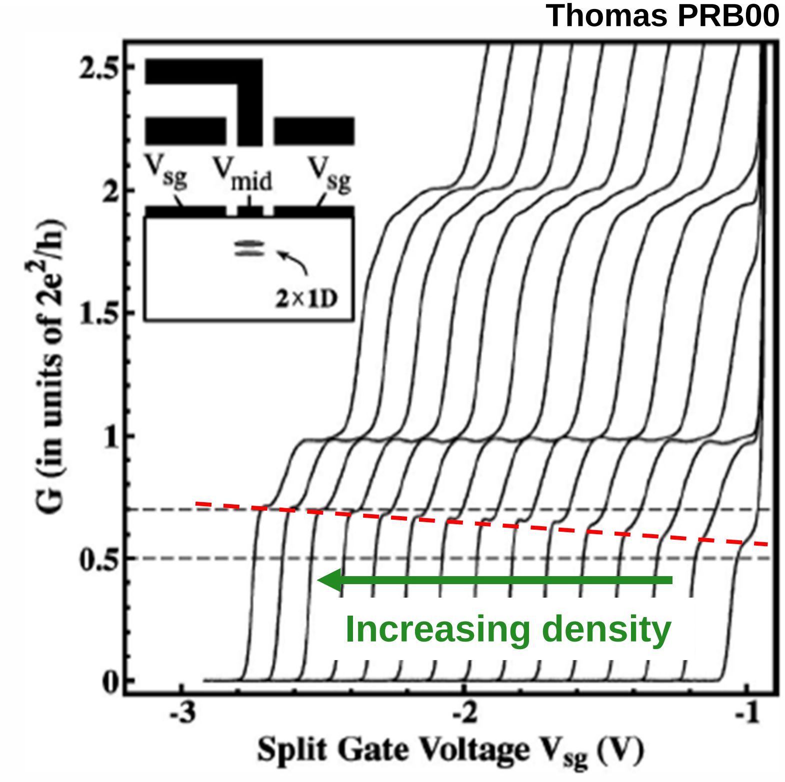

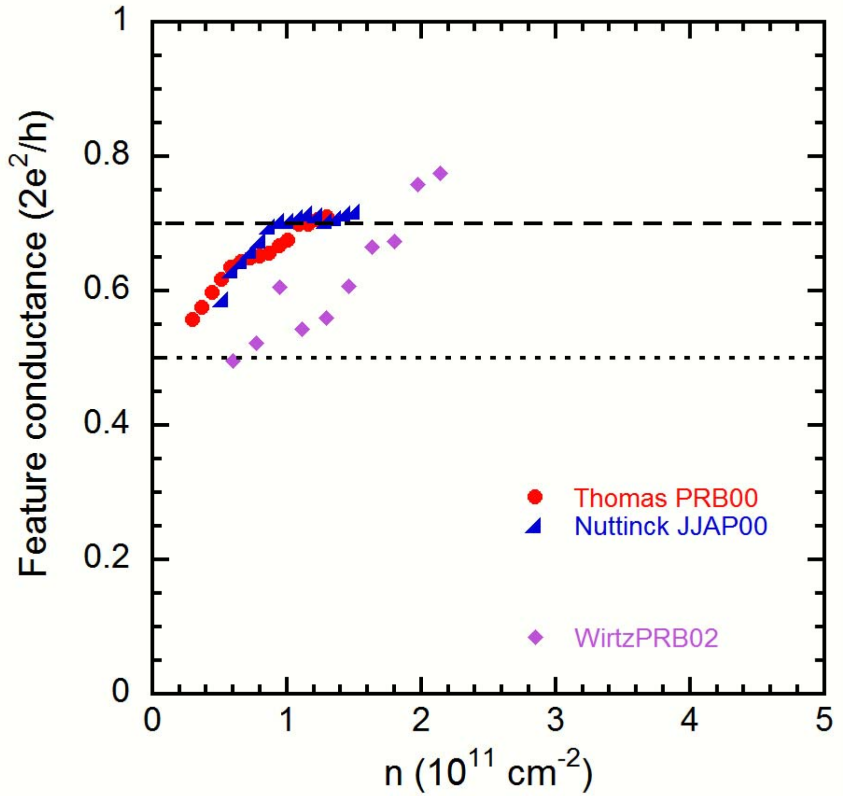

See K.J. Thomas *et al*., PRB 61, 13365 (2000); S. Nuttinck *et al*., JJAP 39, L655 (2000); R. Wirtz *et al*., PRB 65, 233316 (2002).

0.7 with density is a mystery

- **Sometimes the 0.7 plateau falls with increasing density…**

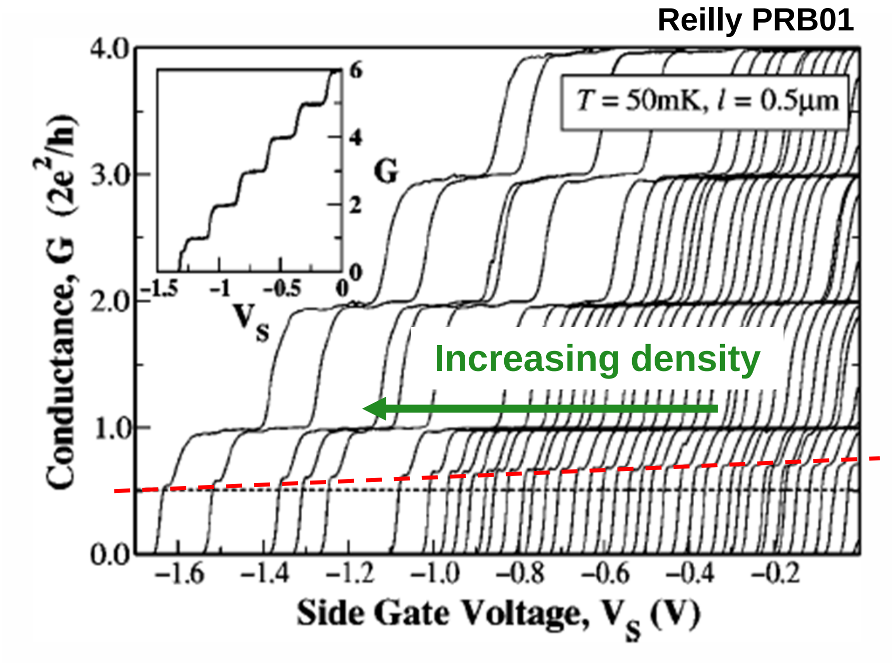

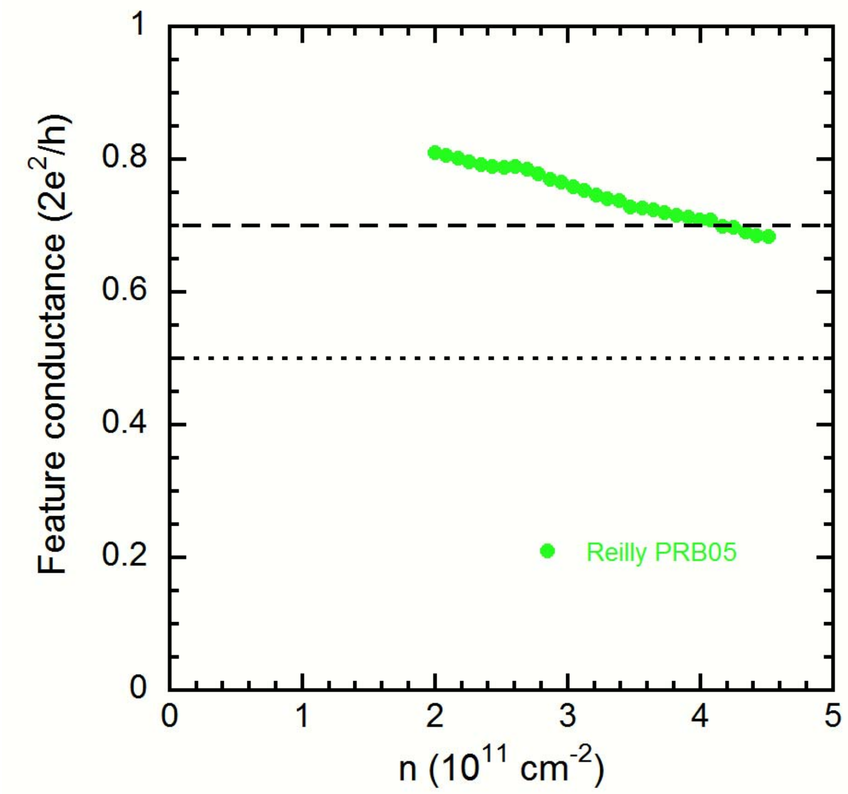

See D.J. Reilly *et al.*, PRB <u>63</u>, 121311 (2001); D.J. Reilly, PRB <u>72</u>, 033309 (2005).

0.7 with density is a mystery

- **And sometimes, the 0.7 plateau even does both!**

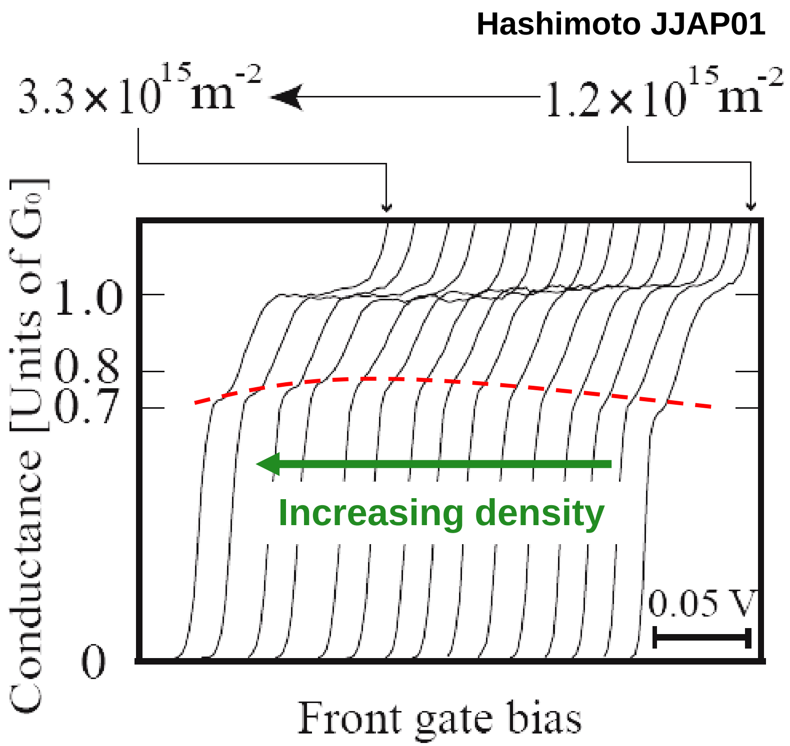

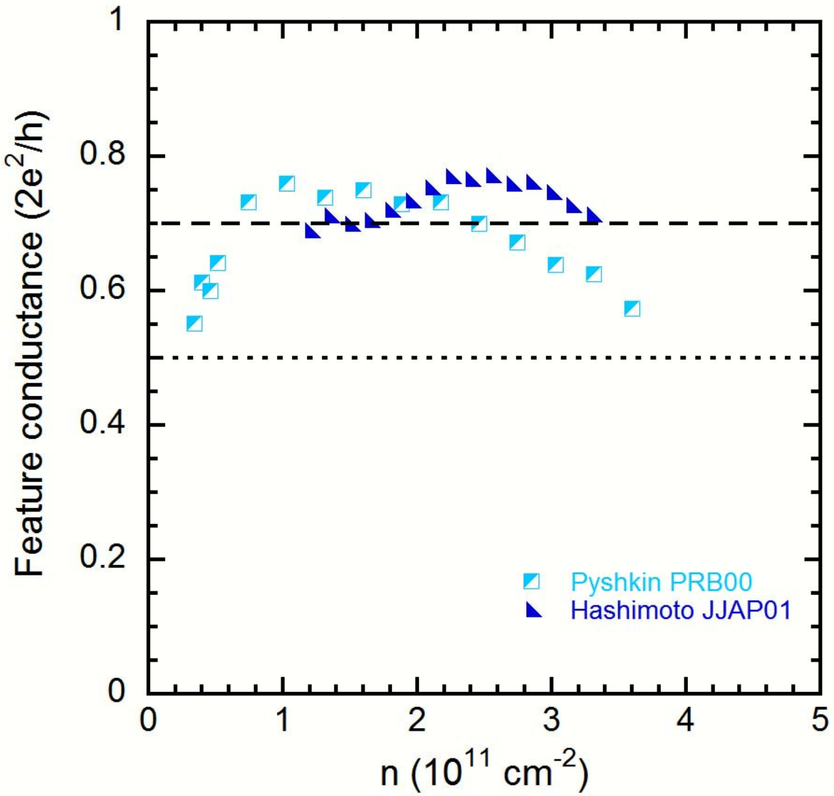

See K. Pyshkin *et al.*, PRB 62, 15842 (2000); K. Hashimoto, JJAP 40, 3000 (2001).

0.7 with density is a mystery

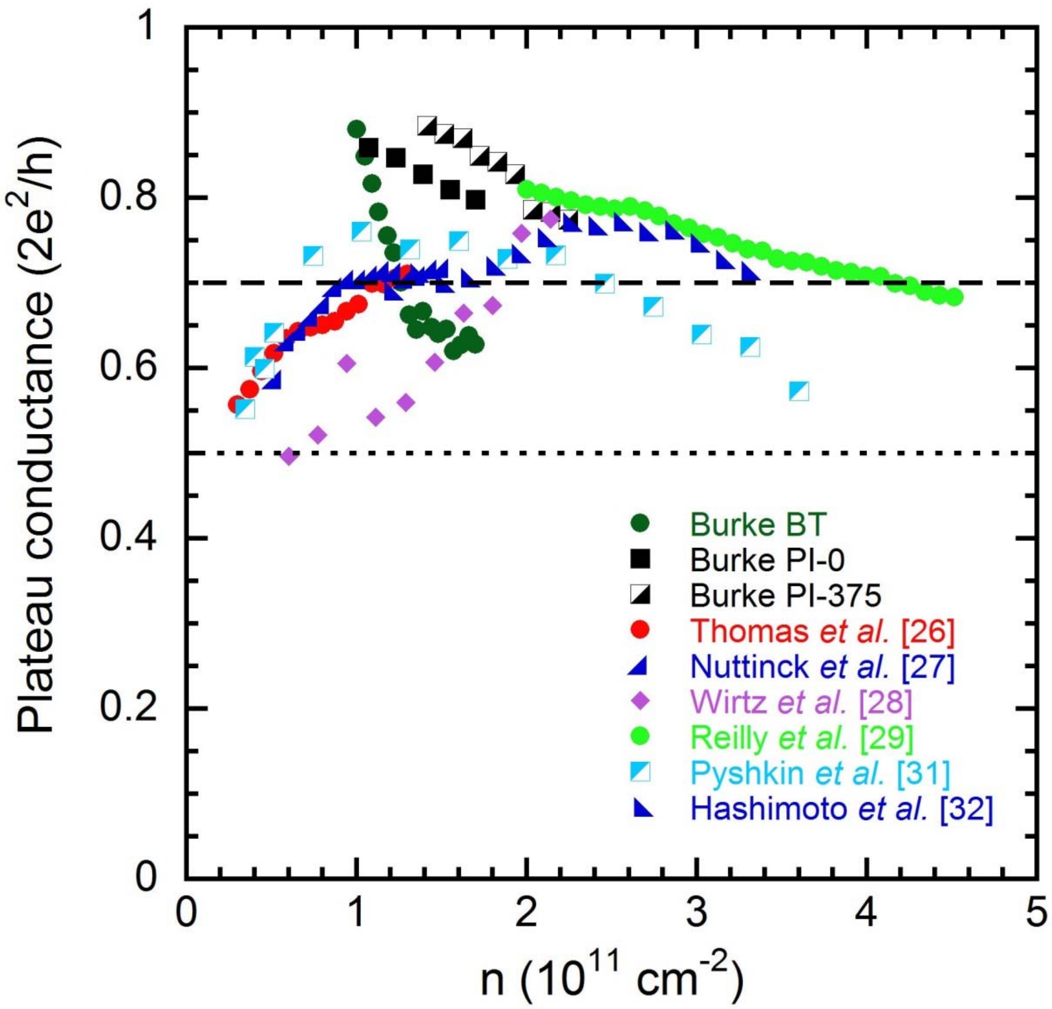

A.M. Burke *et al.*, Nano Lett. *in press*. doi: 10.1021/nl301566d

A more recent study on density and 0.7

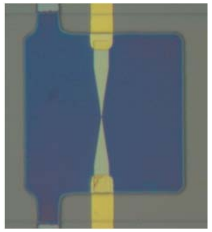

$n_{2D} = 1.83 \times 10^{11}$ cm^{-2}
$\mu = 2.75 \times 10^{6}$ cm^2/Vs
QPC = 0.5 × 0.3 μm

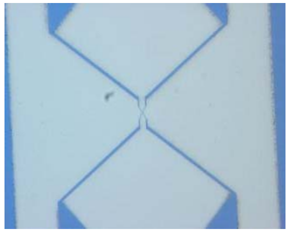

PI-0 / PI-375

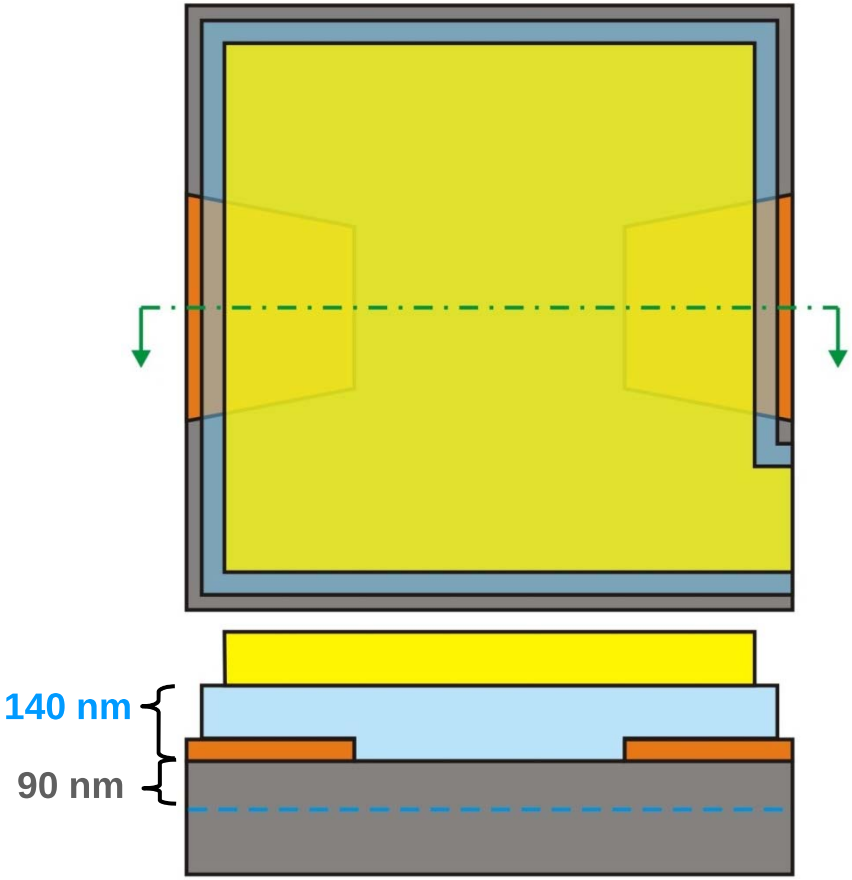

BT

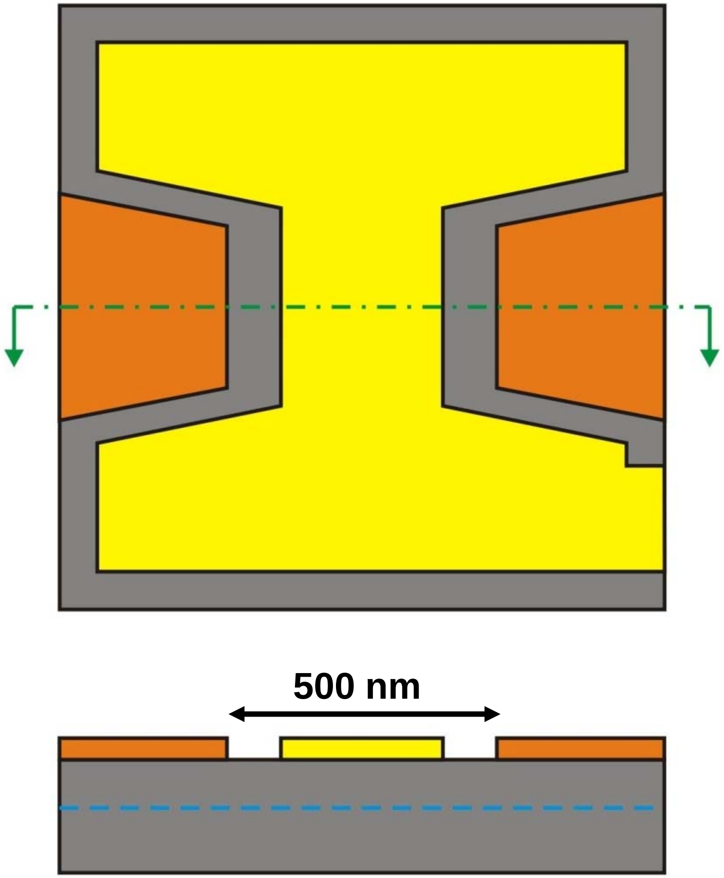

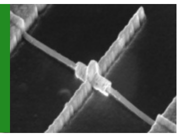

Varying the opening rate γ

- **In the Reilly model, the opening rate γ is linked to the 1D-2D mismatch.**
- **Since the 2D system is quasi-continuum, this is basically tied to the 1D subband spacing. For 0.7, this should be the lowest 1D subband spacing $\Delta E_{1,2}$, in particular.**

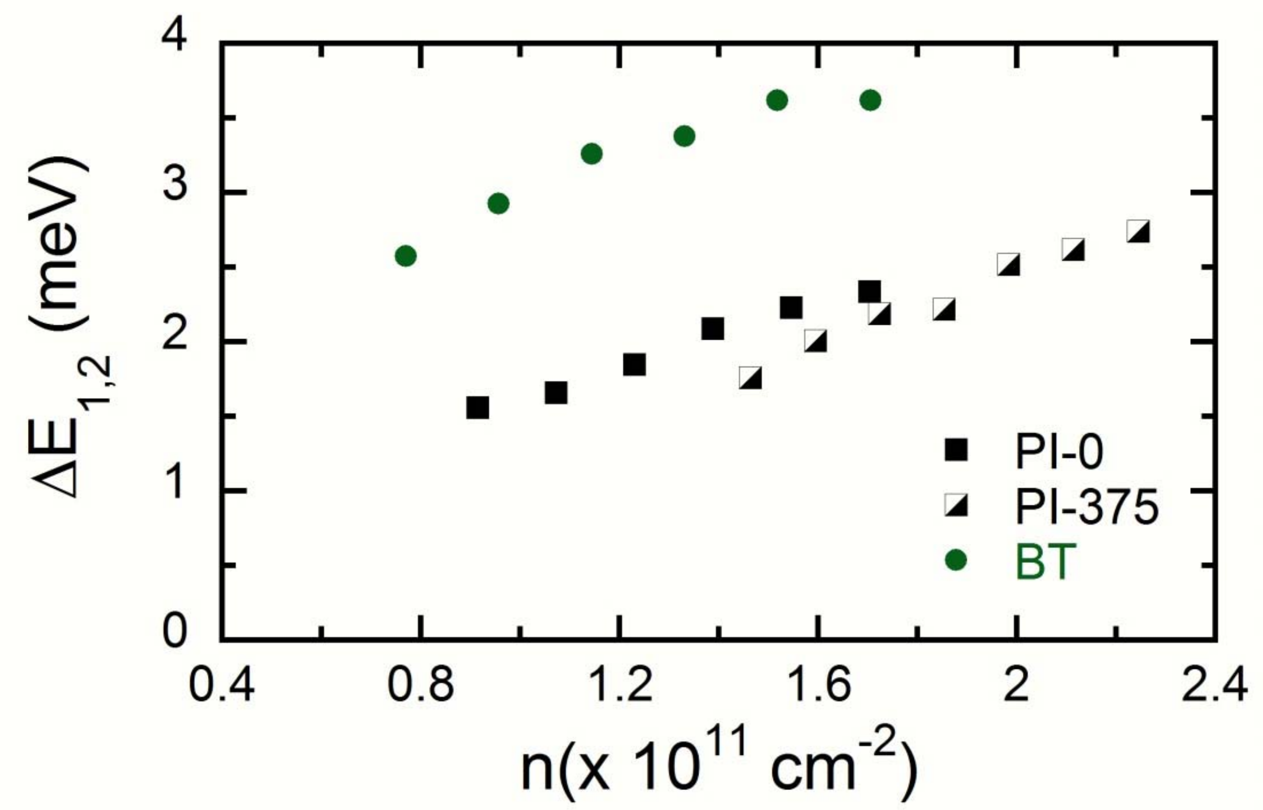

Stronger 1D confinement

and

greater 1D-2D mismatch

A.M. Burke *et al.,* Nano Lett. *in press*. doi: 10.1021/nl301566d

What does 0.7 do in these three devices?

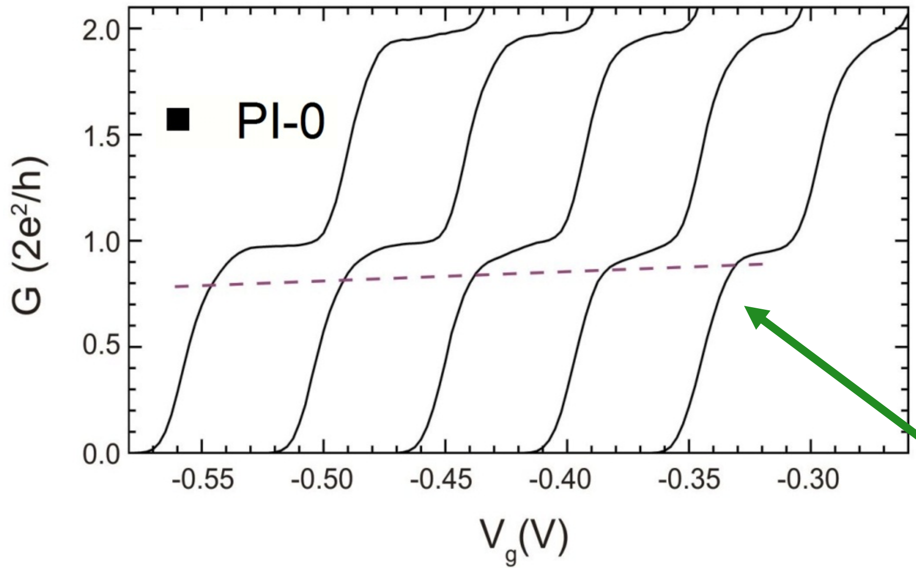

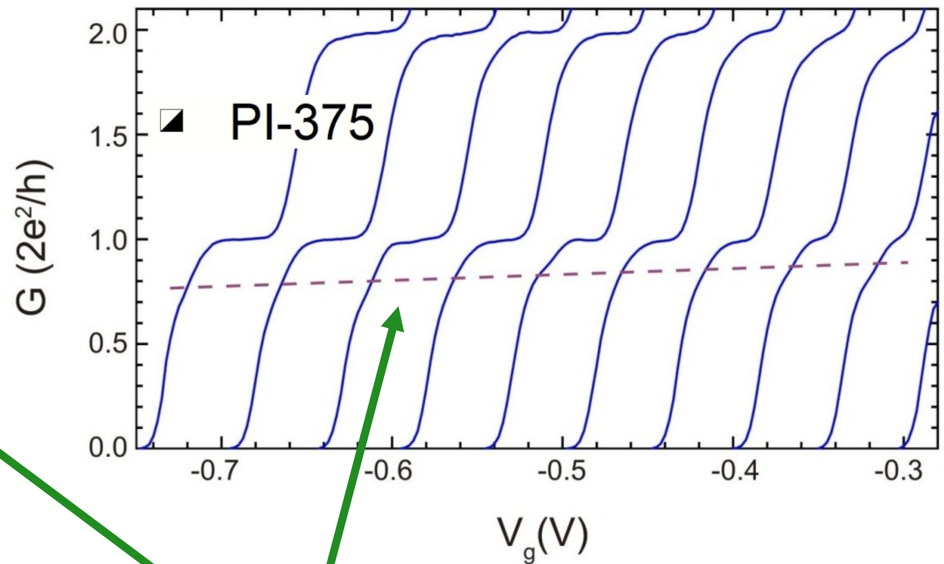

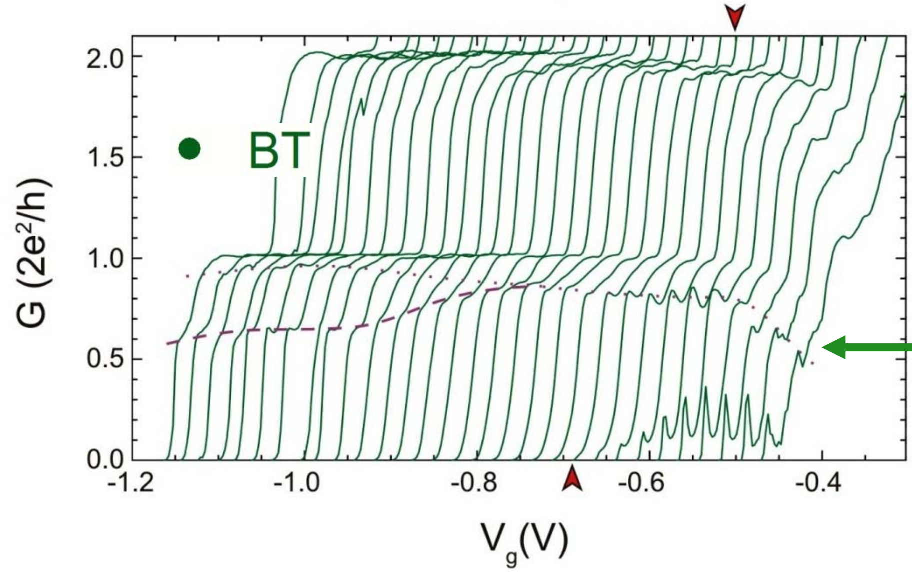

Weaker plateau at higher conductance, slight shift downwards with increasing density.

Strong plateau at lower conductance, with smooth evolution from about 0.7 towards 0.5 with increasing density.

A.M. Burke *et al.*, Nano Lett. *in press*.

Connecting back to density-dep. spin-gap

■ PI-0

◪ PI-375

● BT

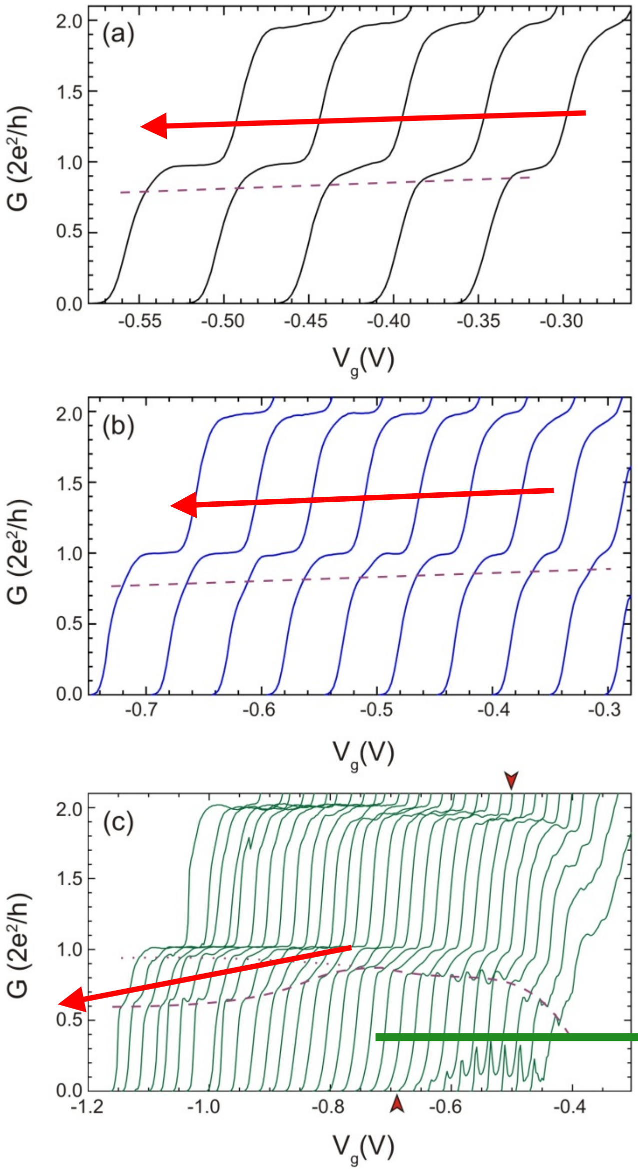

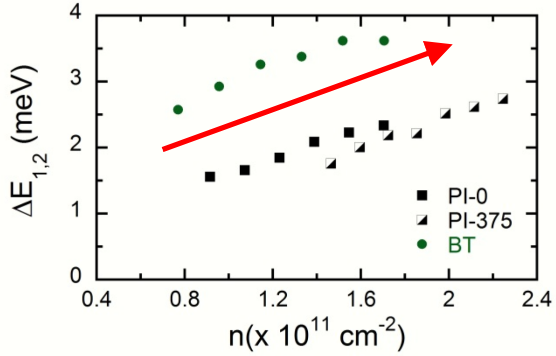

We see a clear correlation between plateau position and evolution and 1D-2D mismatch.

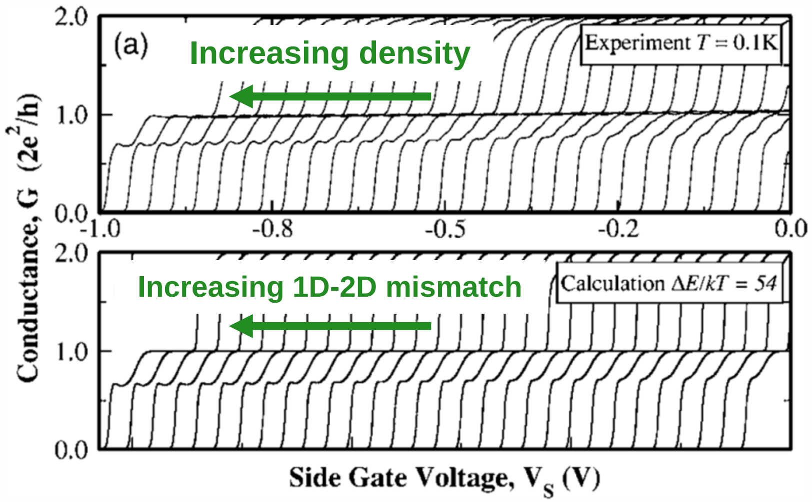

See D.J. Reilly, PRB 72, 033309 (2005).

Smooth evolution from about 0.7 towards 0.5 with increasing density.

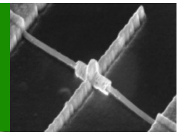

Back to exchange enhancement for a moment

The lowest 1D subband *g**
sits below the trend.

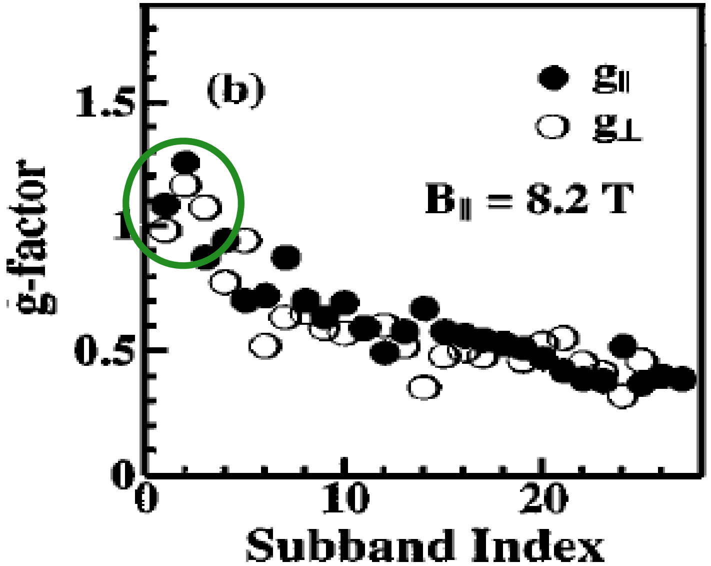

K.J. Thomas *et al.*, PRL 77, 135 (1996).

The lowest 1D subband *g**
sits above the trend.

InGaAs/InP

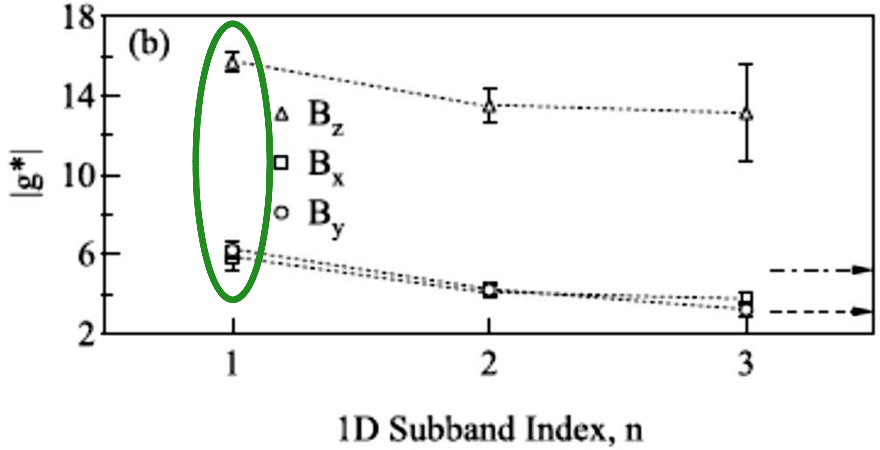

T.P. Martin *et al.*, PRB 81, 041303 (2010).

Back to exchange enhancement for a moment

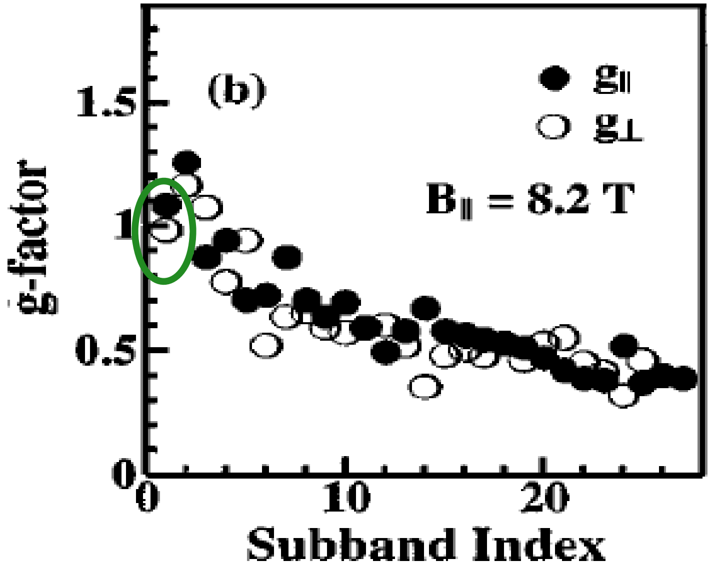

K.J. Thomas *et al.*, PRL 77, 135 (1996).

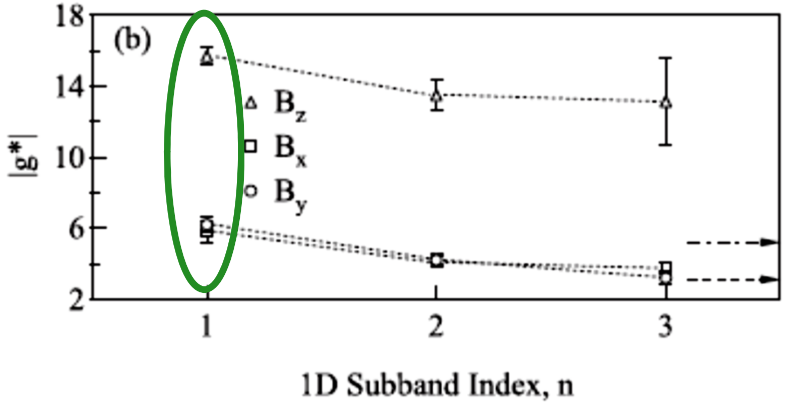

T.P. Martin *et al.*, PRB 81, 041303 (2010).

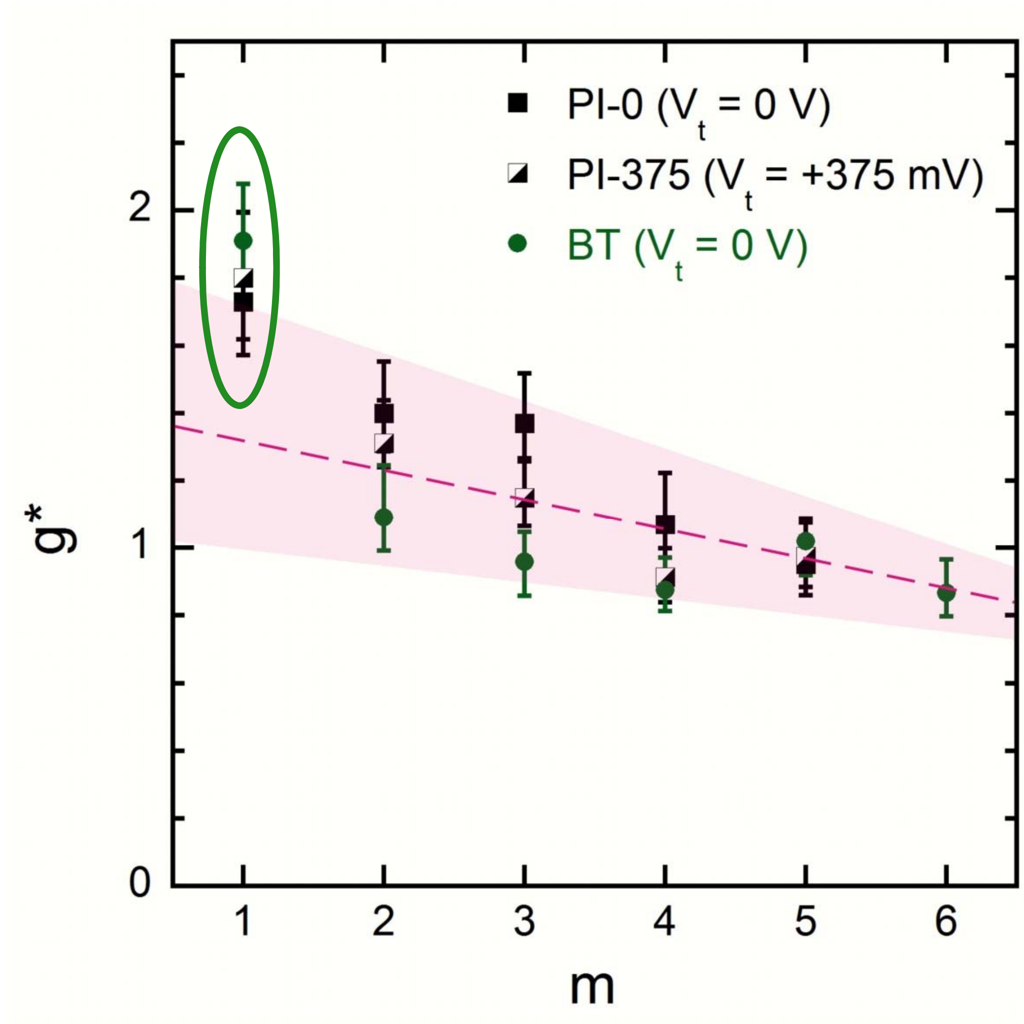

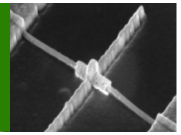

How *g** behaves with density in QPCs

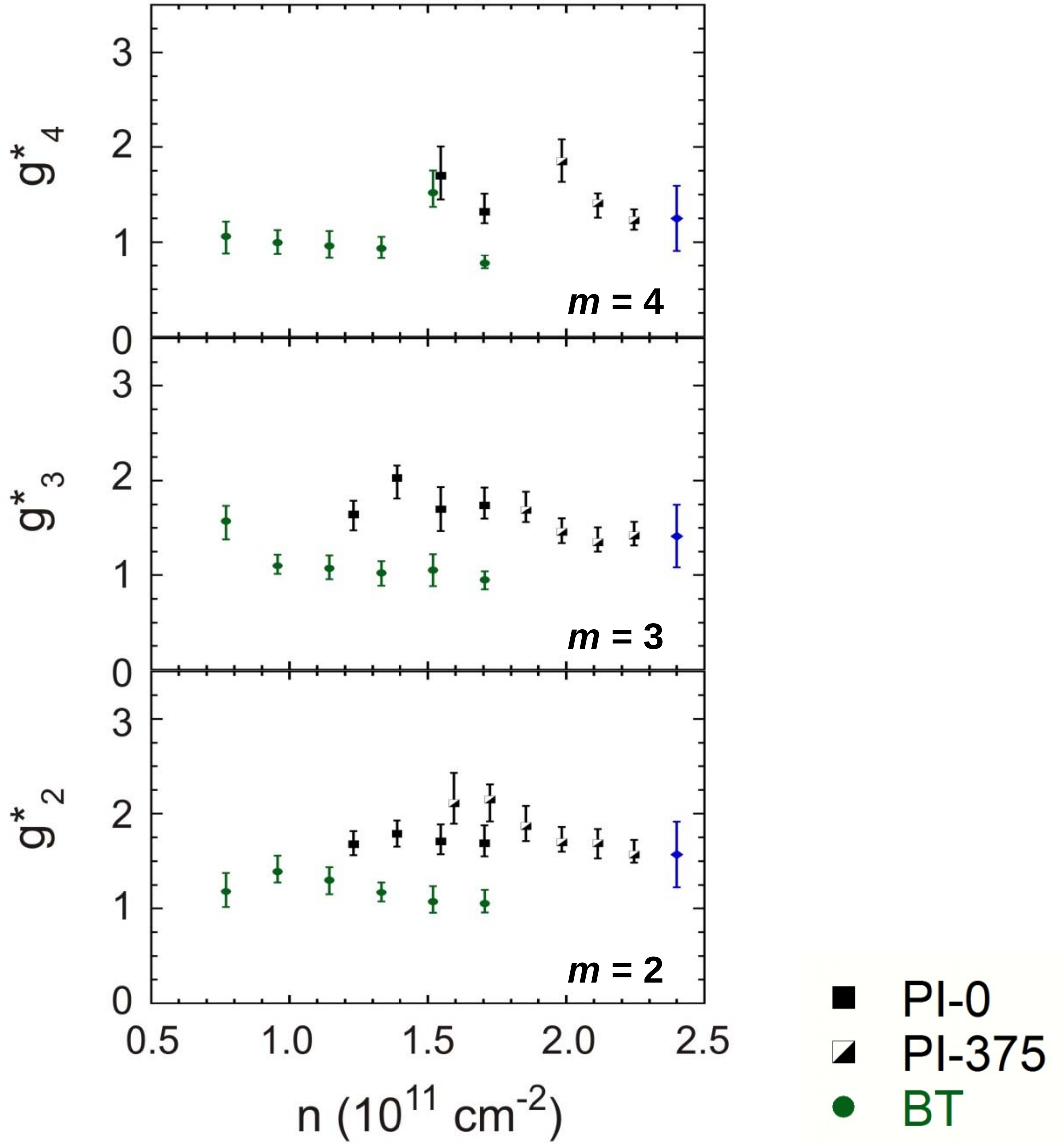

How *g** behaves with density in QPCs

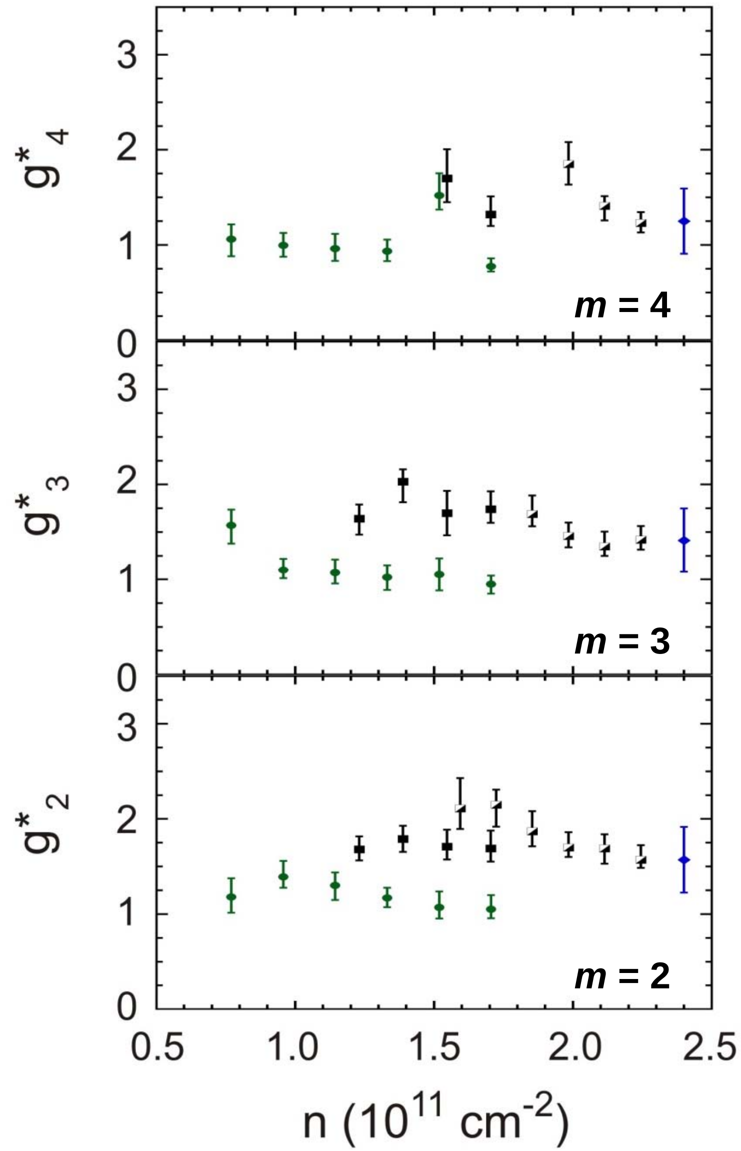

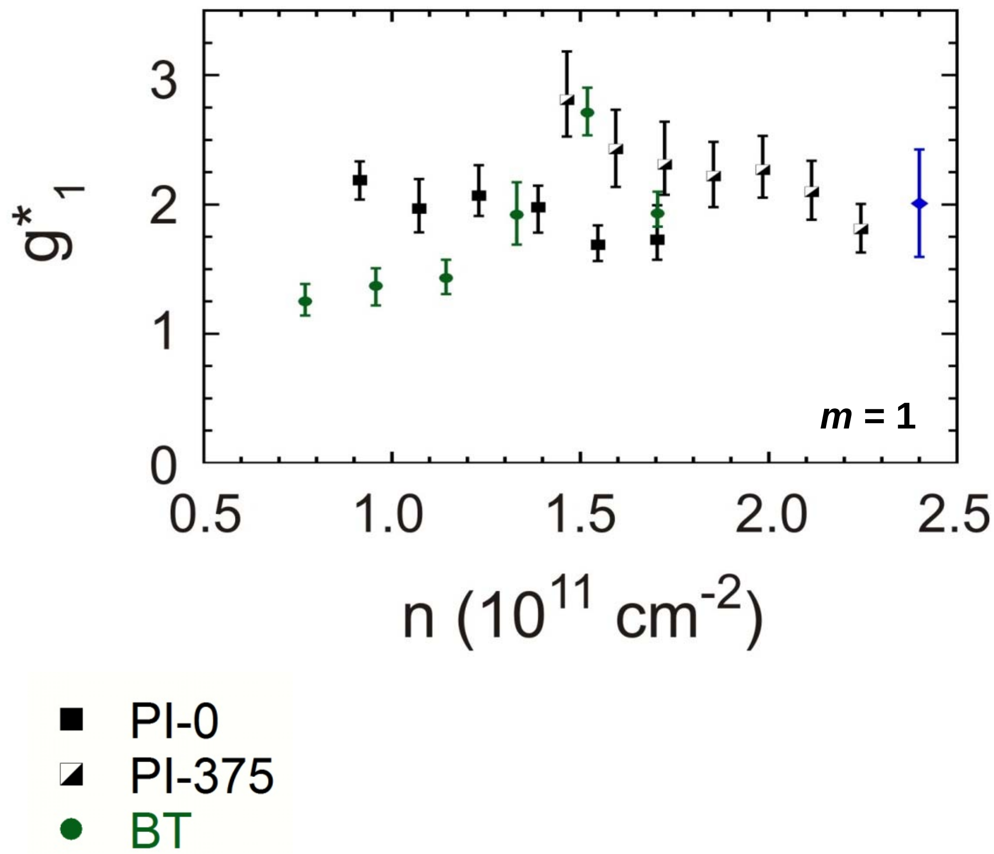

How *g** behaves with density in QPCs

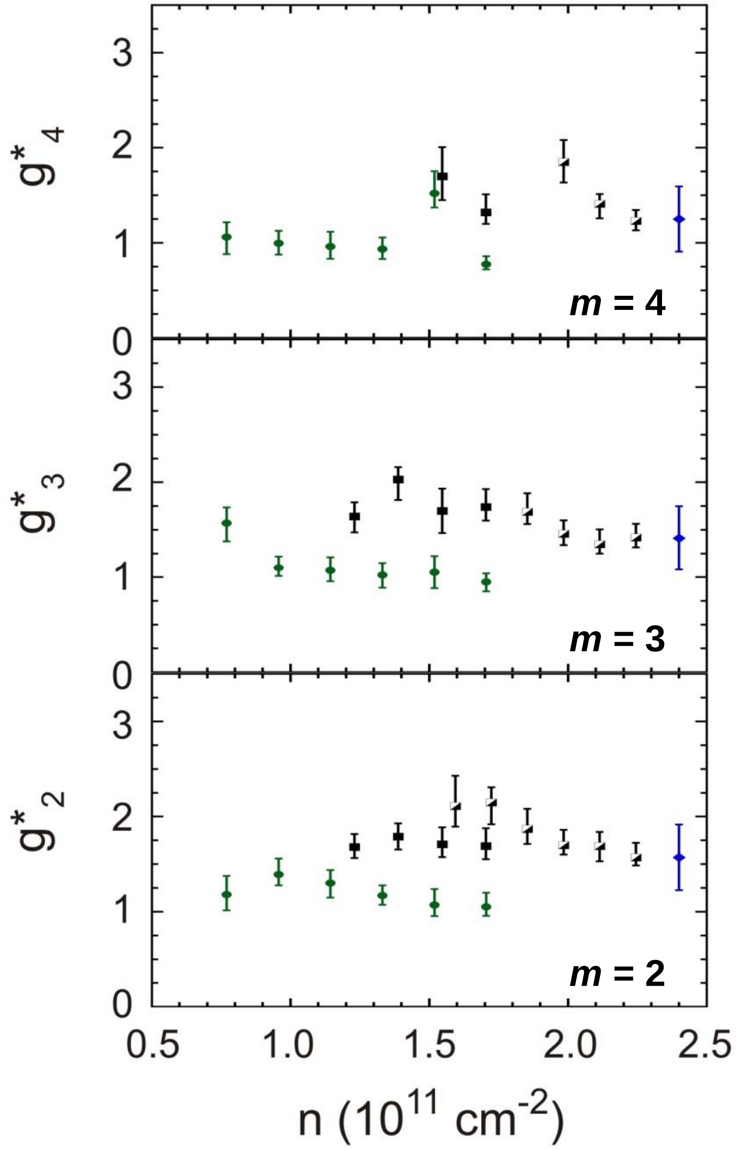

Important implications for spintronics

If QPC potential is managed properly, you can get high *g without going to In or Sb.**

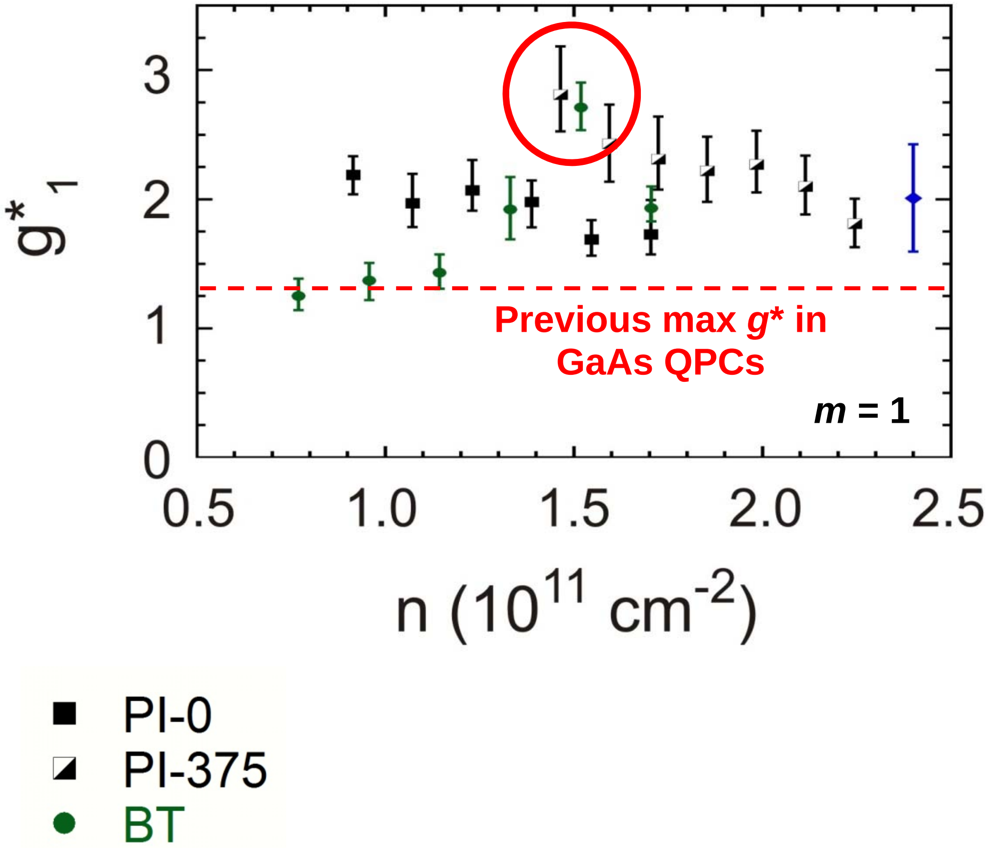

Looking more closely at the subbands

Evolution of the plateaus at high in-plane field

Half plateaus due to breaking of the spin degeneracy of the 1D subbands

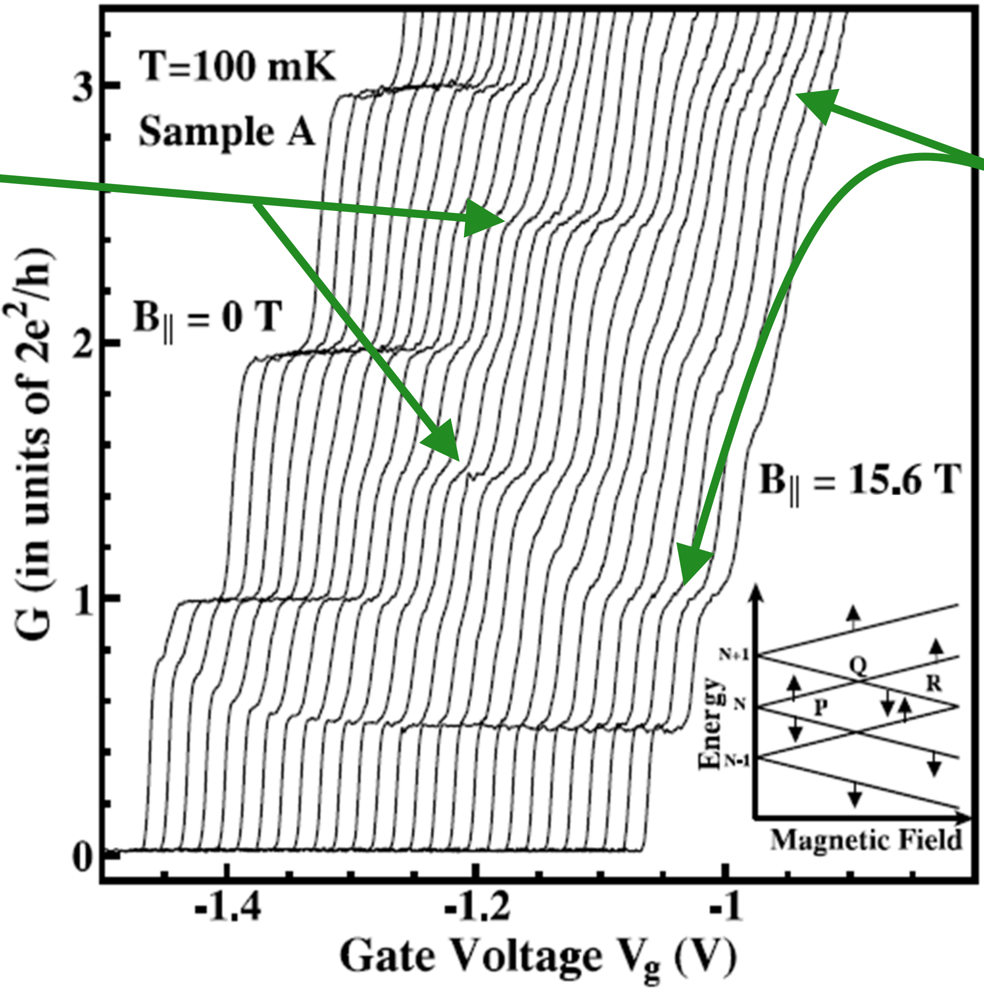

Integer plateaus return due to crossings of the 1D subbands at higher fields

A.C. Graham *et al.,* PRL 91, 136404 (2003).

Visualising the 1D subbands

- **We can see the 1D subbands by plotting the transconductance dG/dV_g versus V_g**

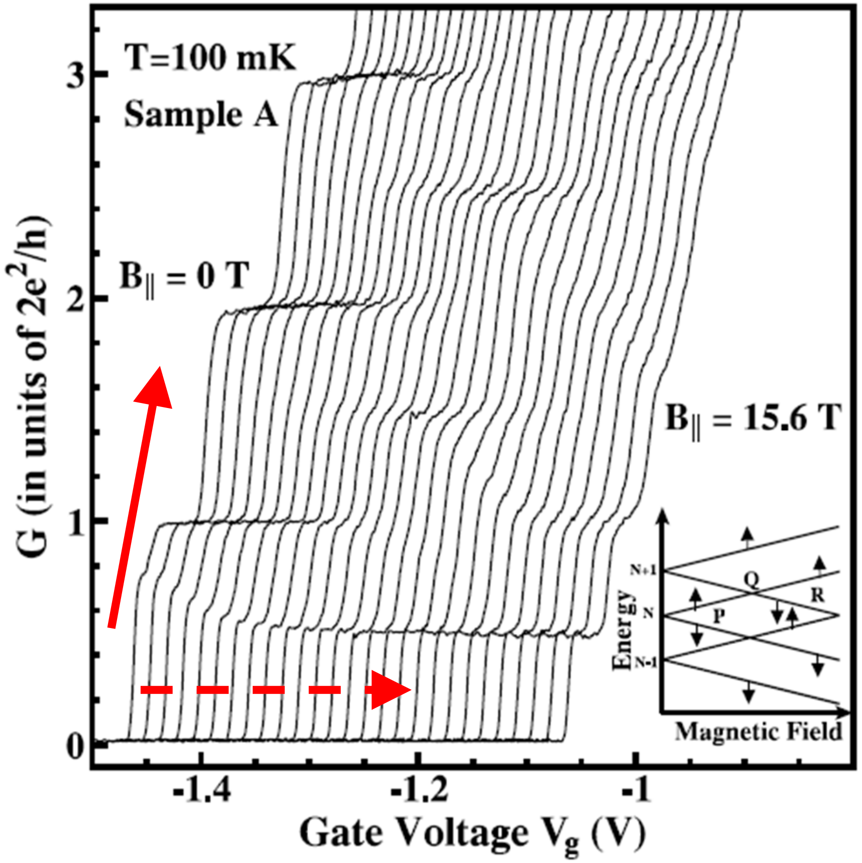

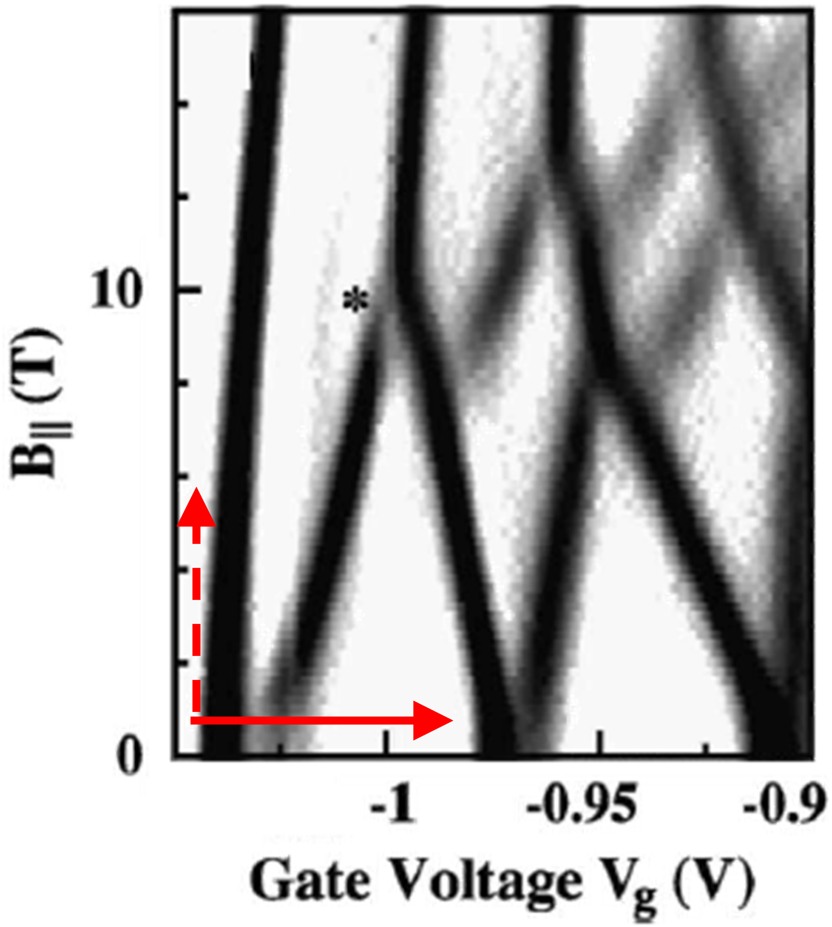

A.C. Graham *et al.*, PRL 91, 136404 (2003).

Nature of the anticrossing

- **Berggren *et al.* used the Kohn-Sham spin-density-functional method, including exchange and correlation effects for an infinite split-gate quantum wire in a parallel, in-plane magnetic field $B_{||}$.**

Note reduced $B_{||}$ with x/c on!

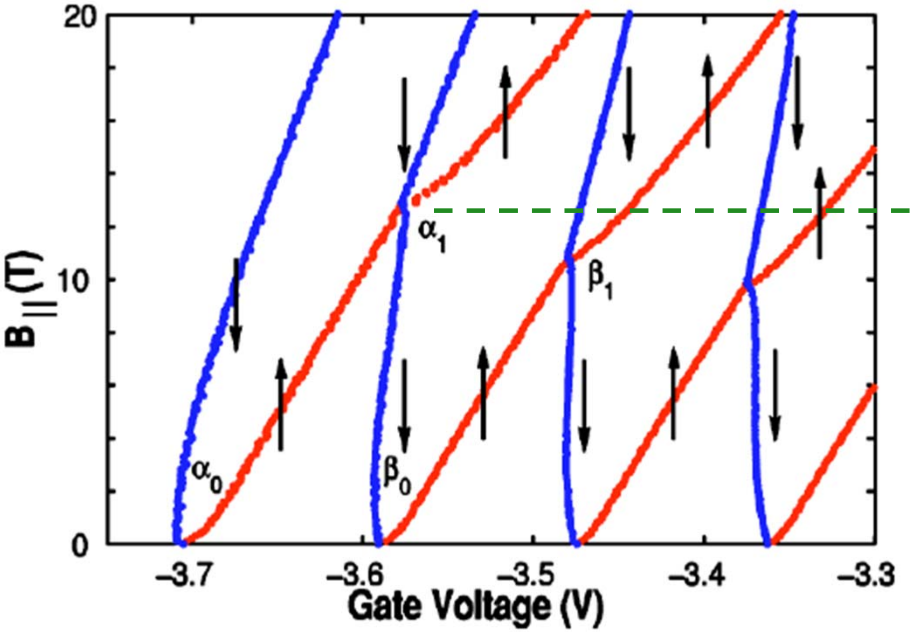

Hartree only

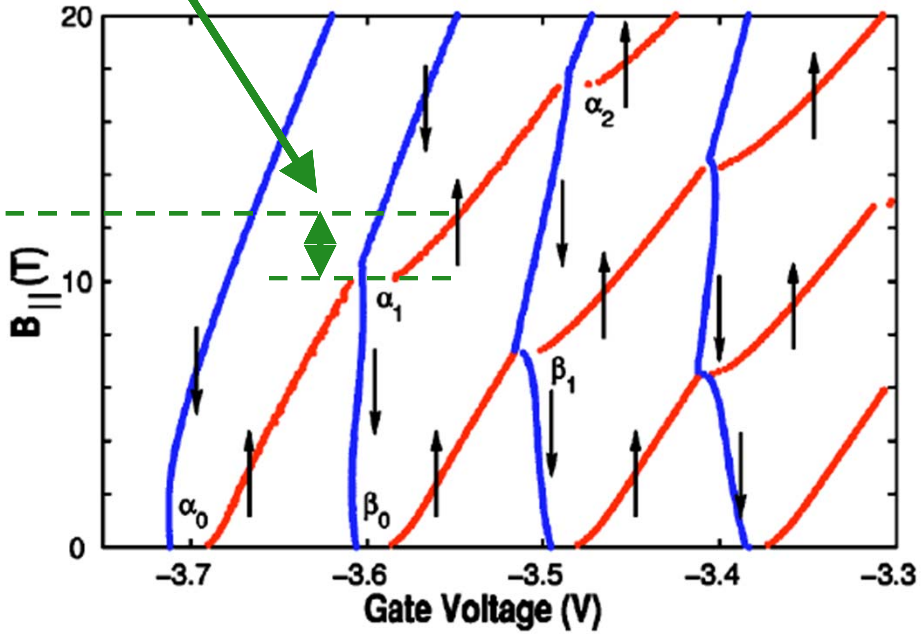

Hartree with exchange and correlation

K.-F. Berggren *et al.*, PRB 71, 115303 (2005).

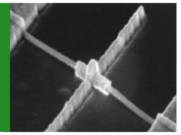

Visualising the 1D subbands

Note the strong anti-crossing in here as 1↑ intercepts the 2↓ subband.

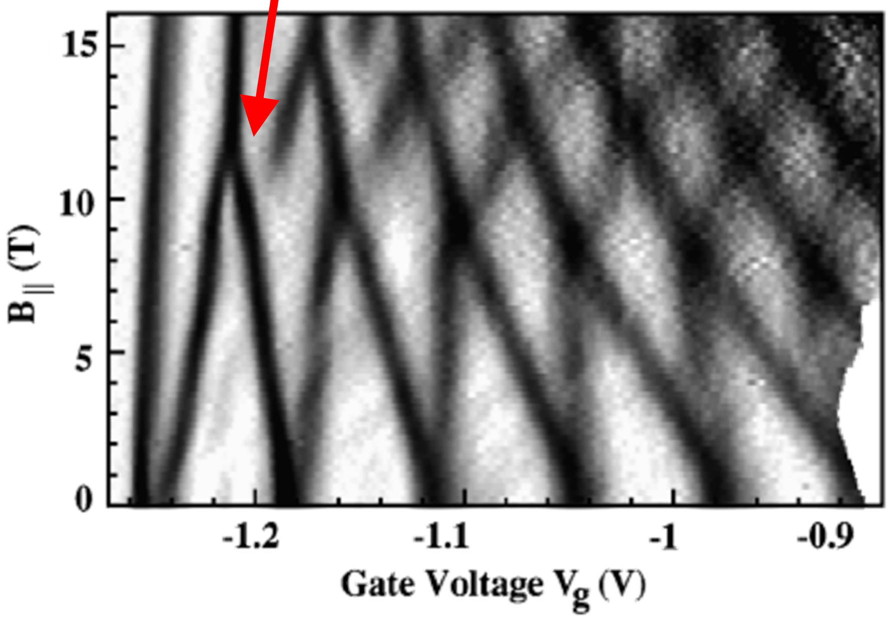

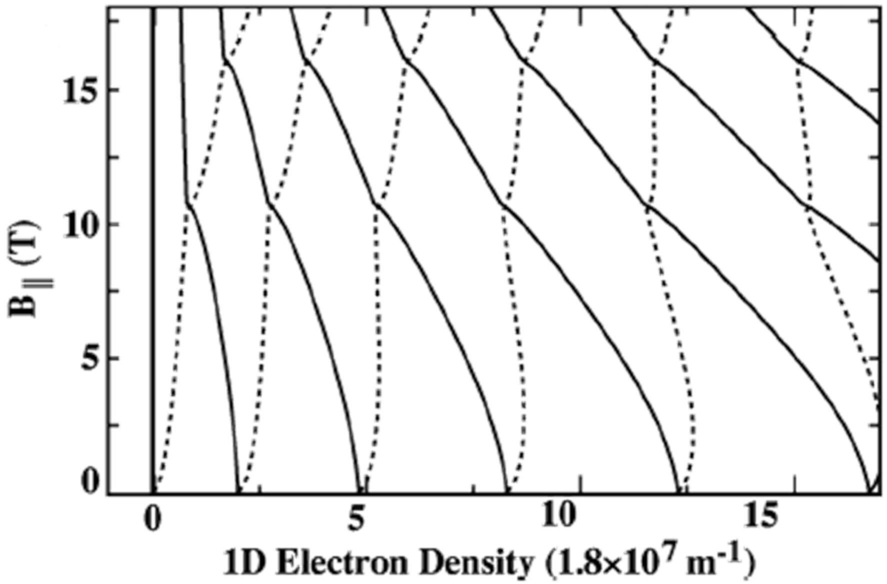

- **Model is for non-interacting electrons in an infinite 1D wire, assuming *g** = 1.9 and parabolic confinement with transverse and vertical (QW) subband spacings of 1.85 and 15 meV respectively. Diamagnetic shift also accounted for (i.e., magnetic confinement).**

A.C. Graham *et al.*, PRL <u>91</u>, 136404 (2003).

0.7 Analogs and 0.7 Complements

The 0.7 plateau would be down here

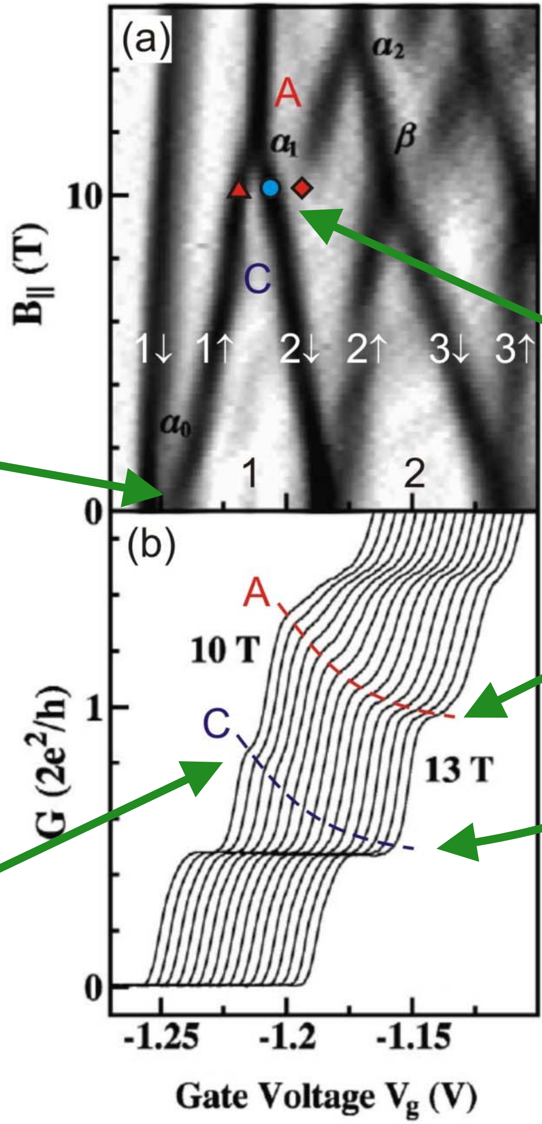

Either side of this anti-crossing there are features that look very much like the 0.7 anomaly.

n.b. this is NOT 0.7, the field is > 10T and not zero!

0.7 Analogs and 0.7 Complements

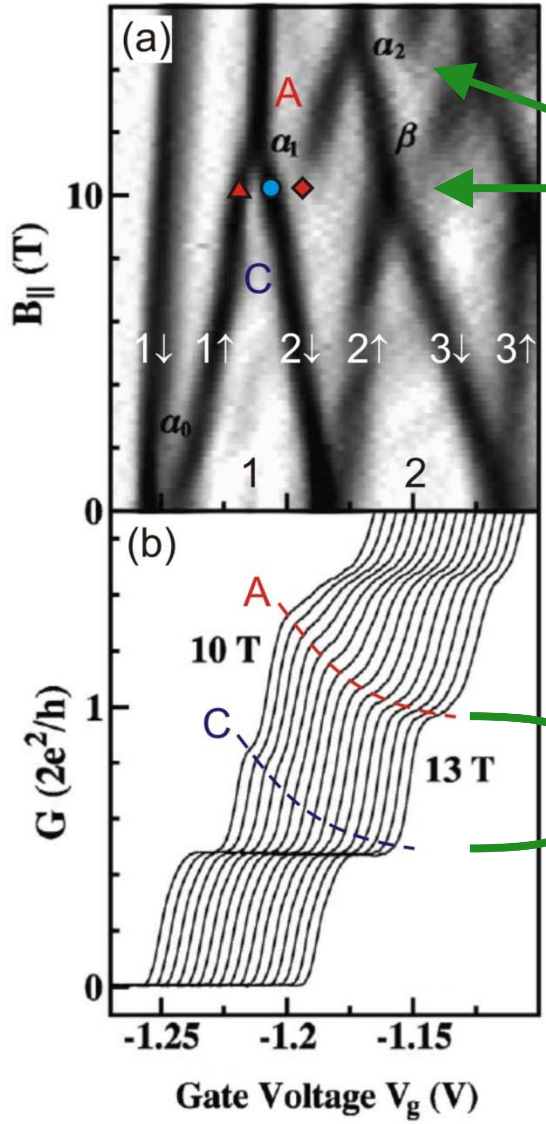

A/C pairs also occur at higher subbands, but they are weaker due to the higher electron density

Separated by a single spin-polarized subband, so the separation is always $0.5G_0$

0.7 Analogs and 0.7 Complements

The 0.7 analog behaves just like 0.7 does as a function of *T*.

But when it collapses to the nearest G_0 at higher field, it behaves like a normal plateau.

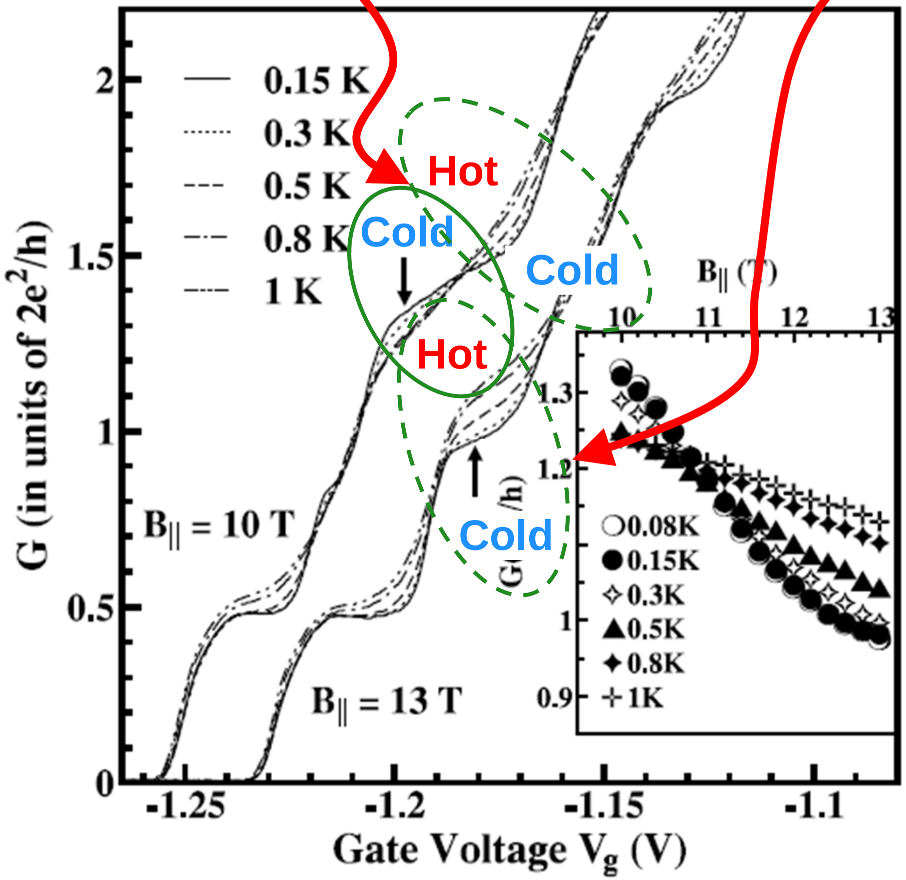

A.C. Graham *et al.*, PRL 91, 136404 (2003).

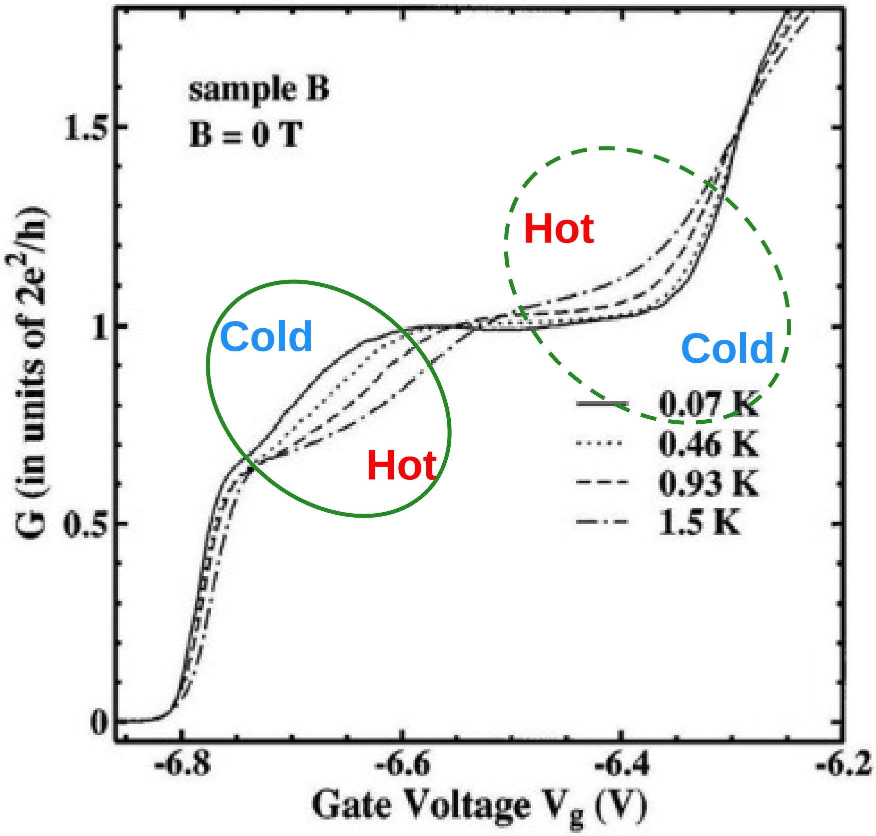

K.J. Thomas *et al.*, PRL 77, 135 (1996).

0.7 Analogs and 0.7 Complements

The dependence has a 'crossover' in in-plane field, and the 0.7 anomaly has the same behaviour.

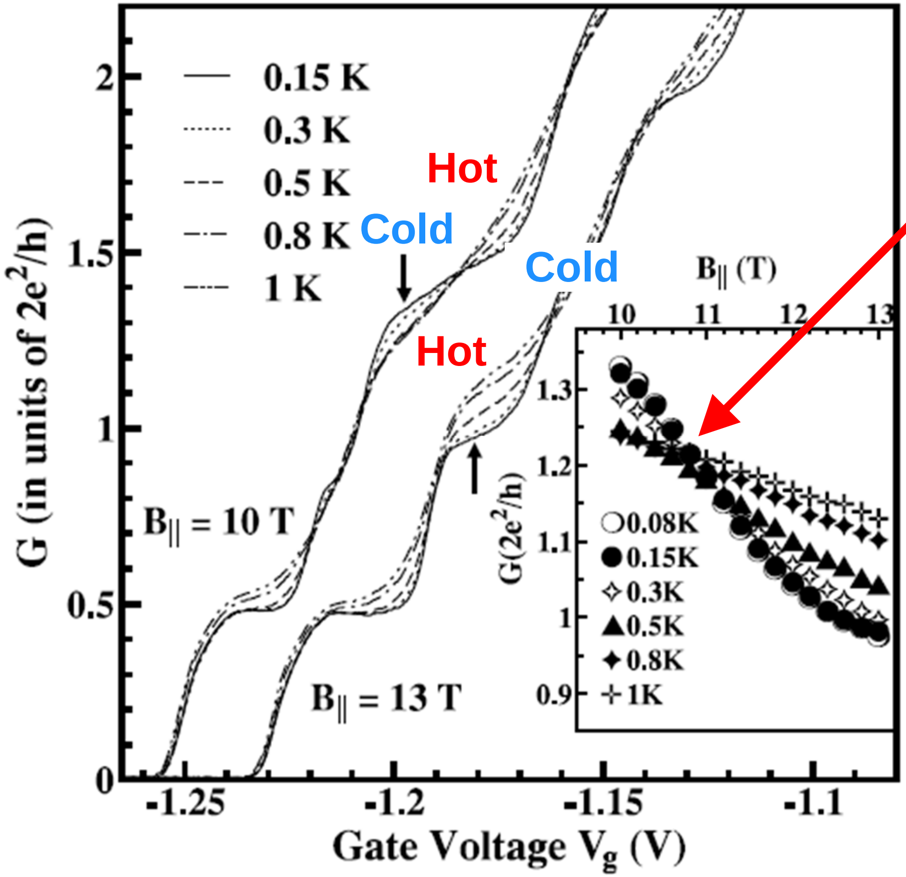

A.C. Graham *et al.,* PRL 91, 136404 (2003).

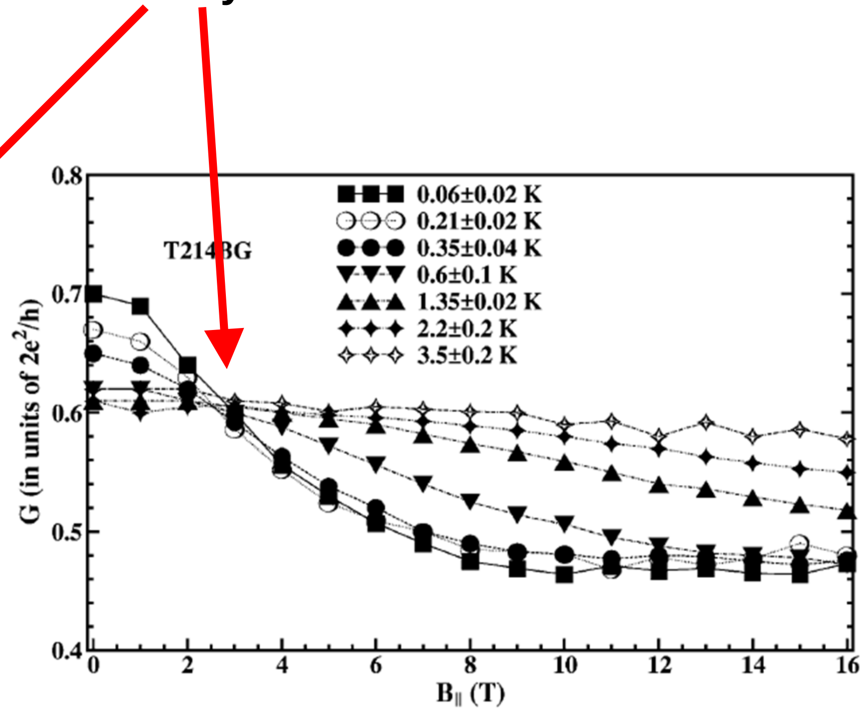

K.J. Thomas *et al.,* Physica E 12, 708 (2002).

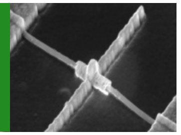

Teasing out what the subbands do at 0.7

- In-plane field $B_{||}$ = 5T to ensure that the 1D subbands are clearly spin-resolved.

The $1_{\downarrow}$ subband does not split until after $|V_{sd}|$ > 0.12 meV.

Splitting rate is also very low

Big gap in where $1_{\downarrow}$ and the other subbands become bias-resolved

Note that $1_{\uparrow}$, and $n_{\uparrow}$ and $n_{\downarrow}$ for $n \geq 2$ split immediately for $|V_{sd}| > 0$

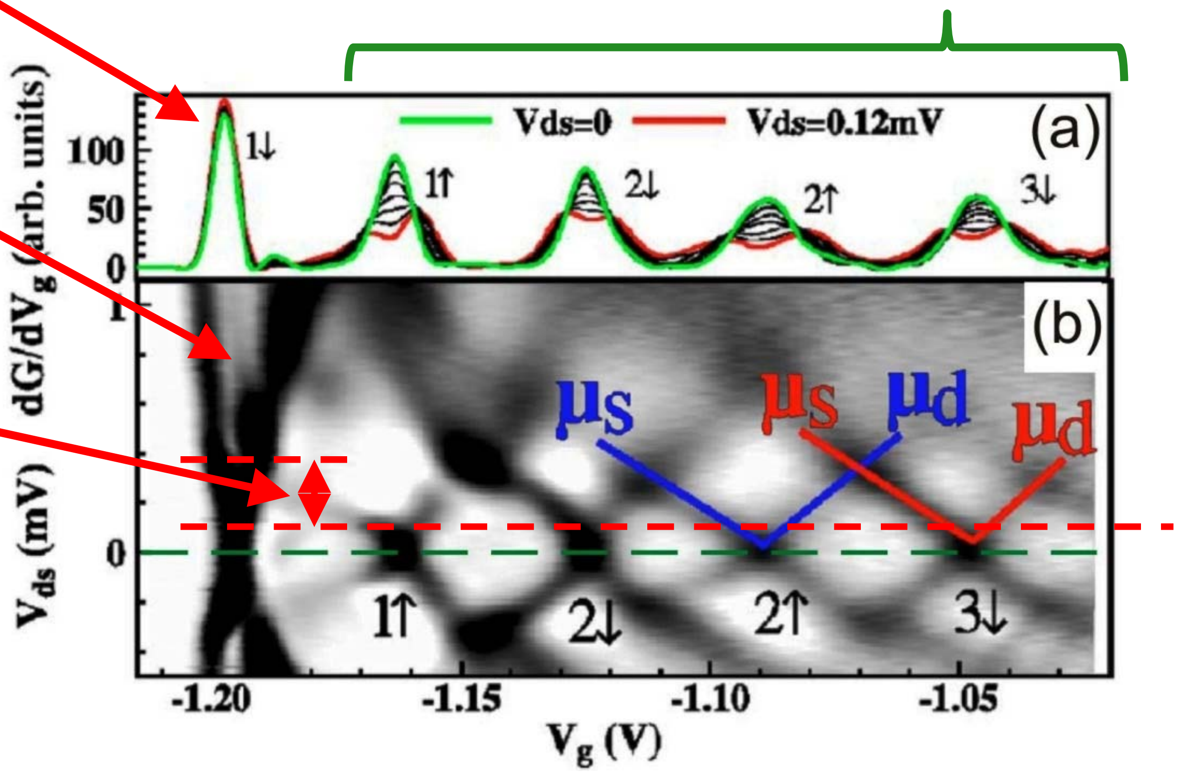

A.C. Graham *et al.,* PRB 72, 193305 (2005).

Teasing out what the subbands do at 0.7

- **The delayed bias-splitting of $1_{\downarrow}$ is interpreted as the $1_{\downarrow}$ subband dropping rapidly in energy as soon as it populates. Splitting is resolved when the population-induced drop is insufficient to reach μ_d.**

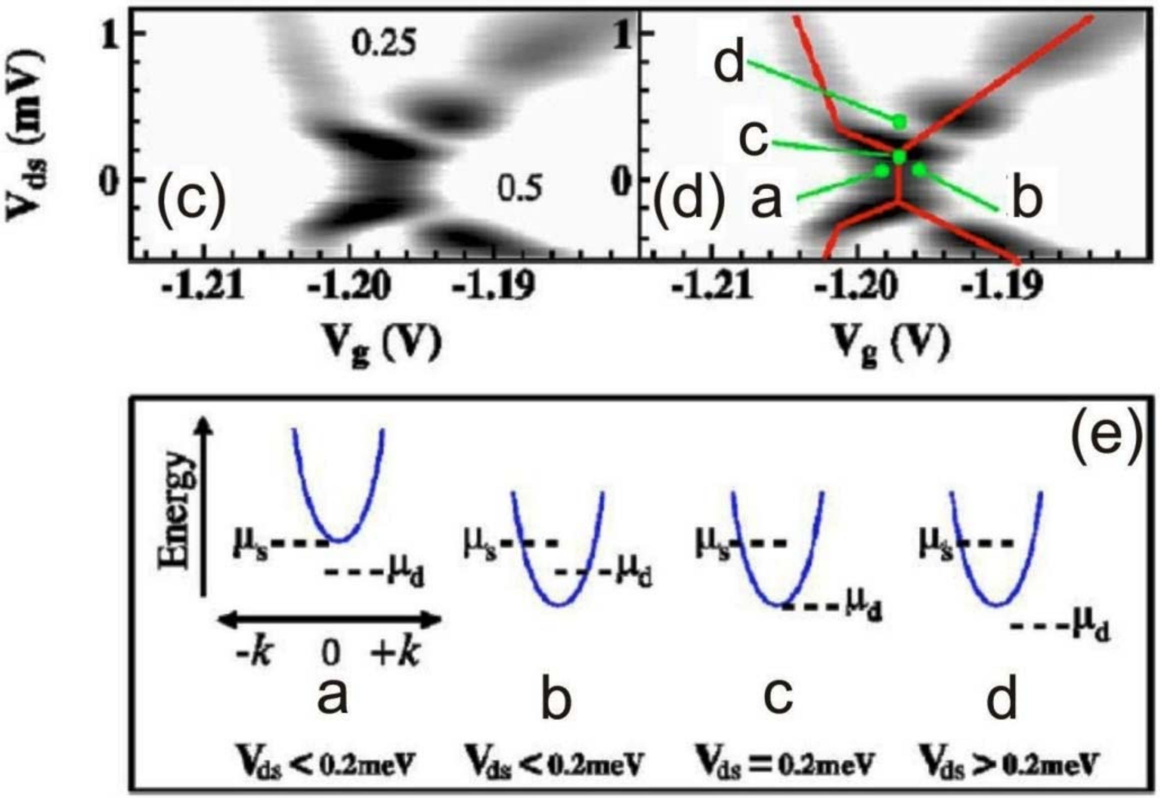

A.C. Graham *et al.*, PRB 72, 193305 (2005).

Teasing out what the subbands do at 0.7

- If we look at $B_{||} = 0$ data near the 0.7 anomaly, we can see there's more to the problem.

The $1_{\uparrow}$ subband appears to be stretched along V_g rather than V_{sd}.

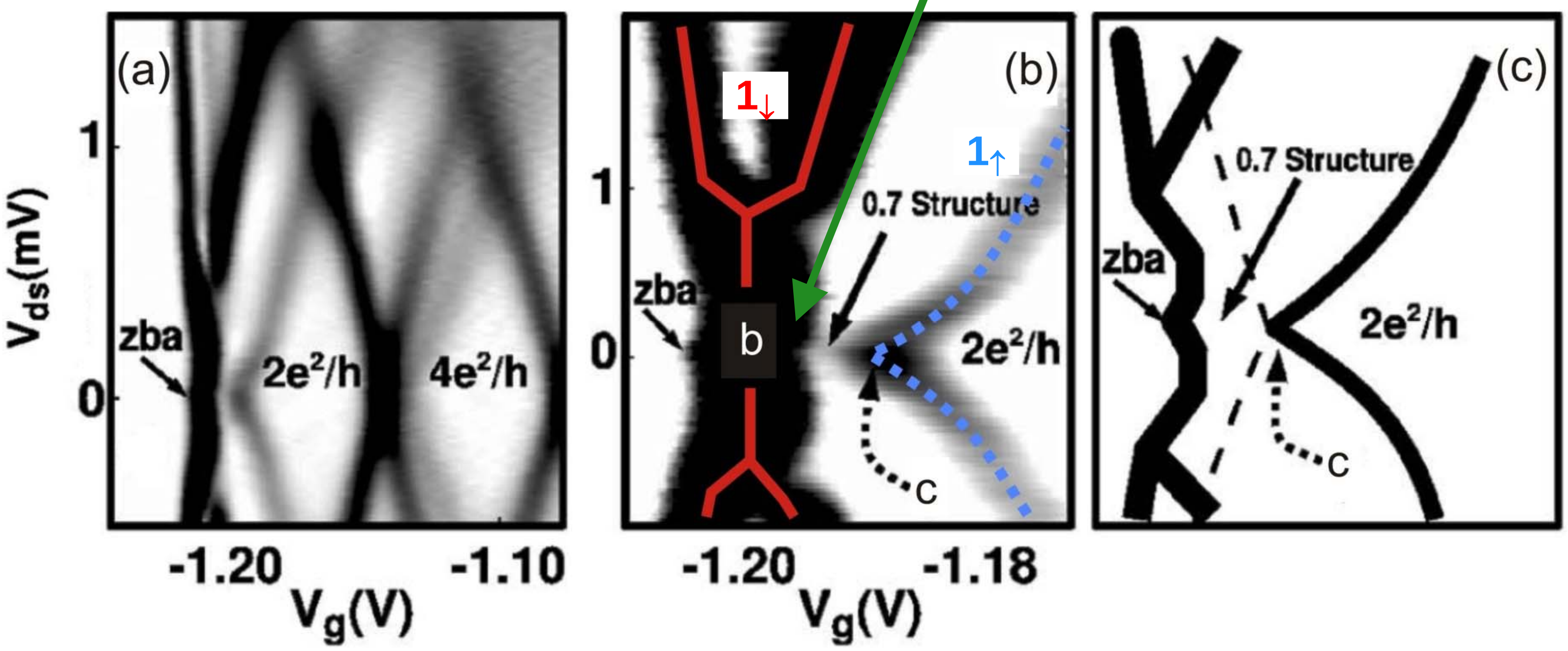

A.C. Graham *et al.*, PRB 75, 035331 (2007).

Teasing out what the subbands do at 0.7

- **We can work out a scenario for the 0.7 data at $B_{||}$ = 0 by going back to high field.**

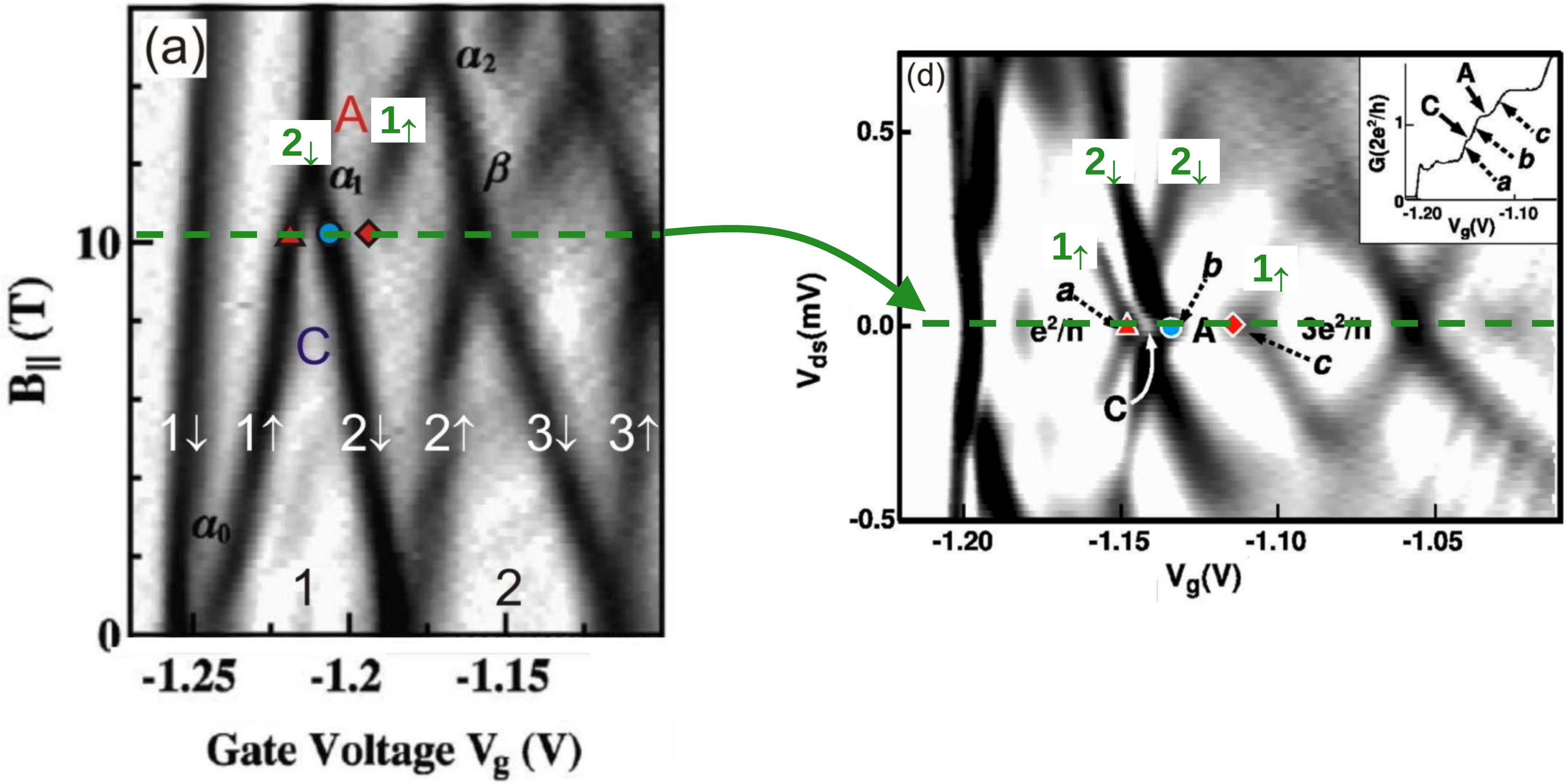

A.C. Graham *et al.*, PRB 75, 035331 (2007).

Teasing out what the subbands do at 0.7

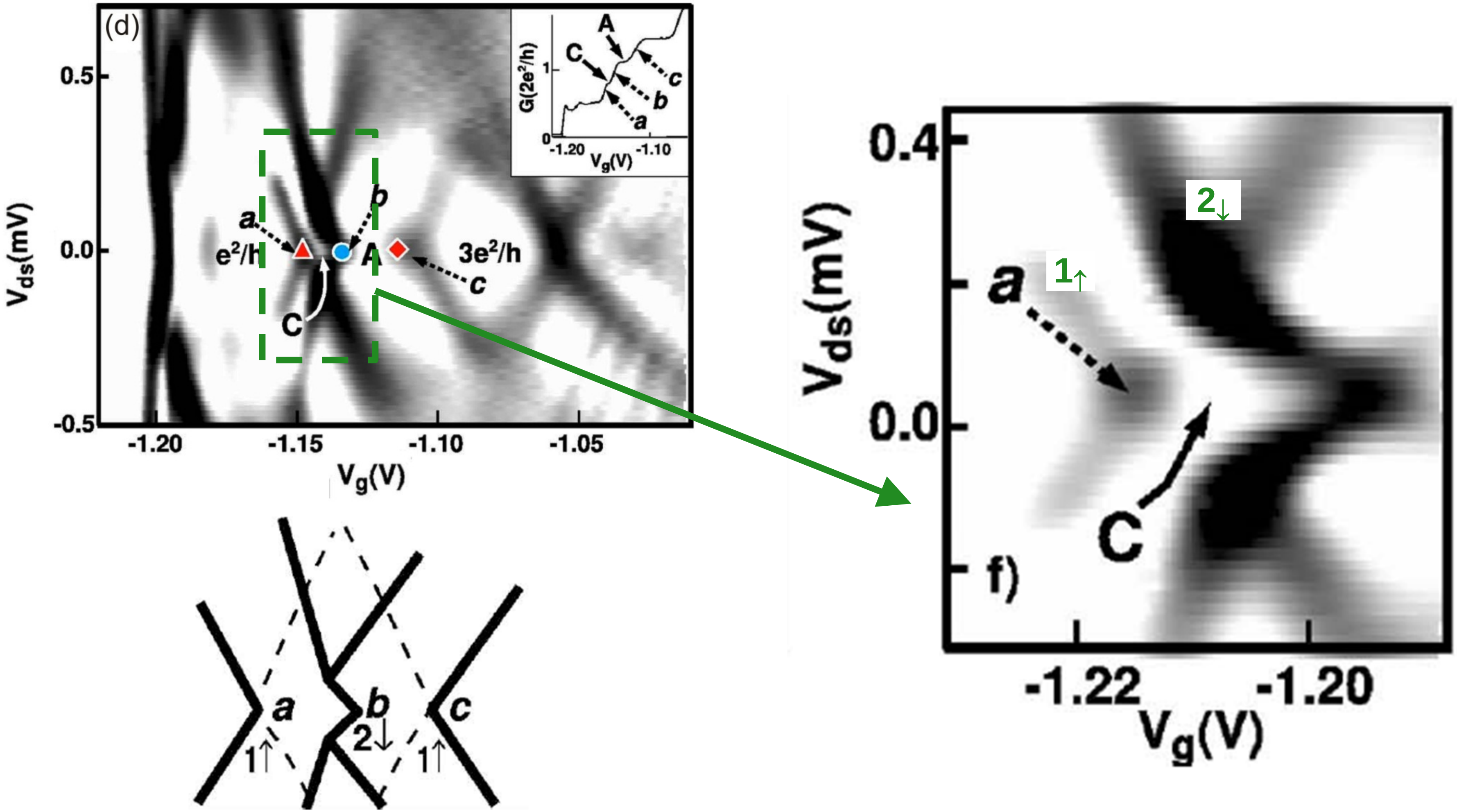

A.C. Graham *et al.*, PRB 75, 035331 (2007).

Teasing out what the subbands do at 0.7

- If you approach point a (i.e., follow the line from i to ii) then $1_{\uparrow}$ coincides with μ.
- And if you approach point c (i.e., follow the line from iv to iii) then $1_{\uparrow}$ coincides with μ.
- The only way this can happen is if $1_{\uparrow}$ is pinned at the chemical potential, while $2_{\downarrow}$ shoots past it.

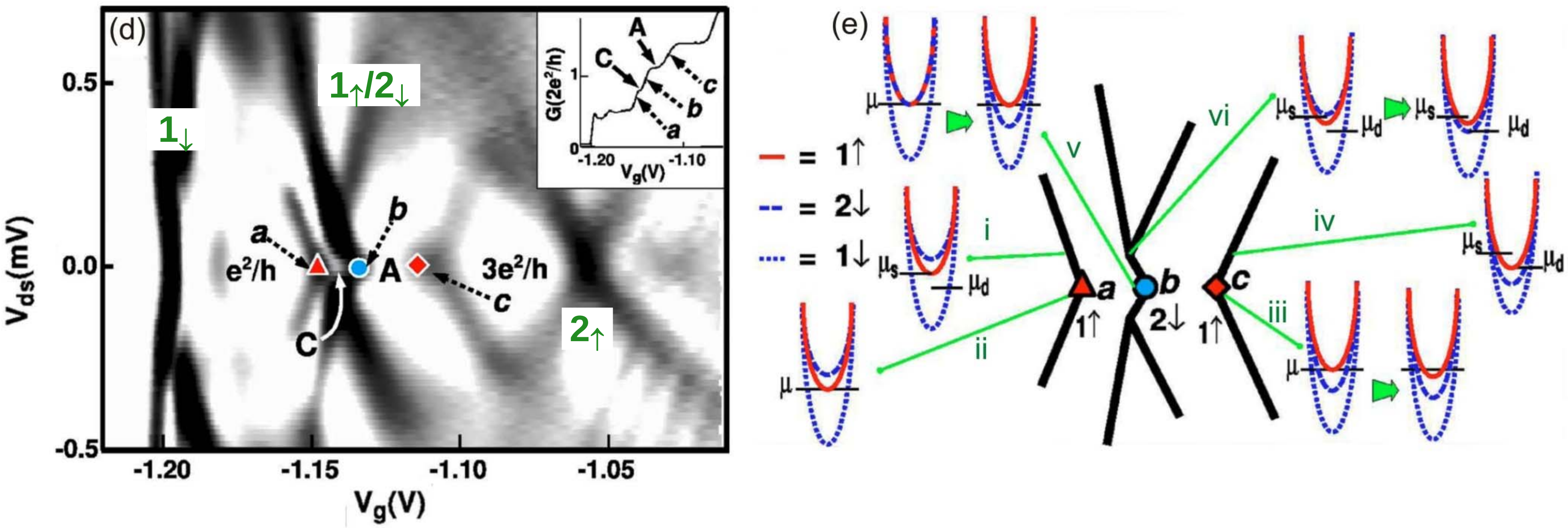

A.C. Graham *et al.,* PRB 75, 035331 (2007).

Teasing out what the subbands do at 0.7

- If we consider the 0.7 data again… first, the spin-degenerate 1st subband reaches μ. When it does, $1_\downarrow$ rapidly drops in energy and $1_\uparrow$ pins, allowing a gap to open, and producing the 0.7 anomaly via a spin-gap model.

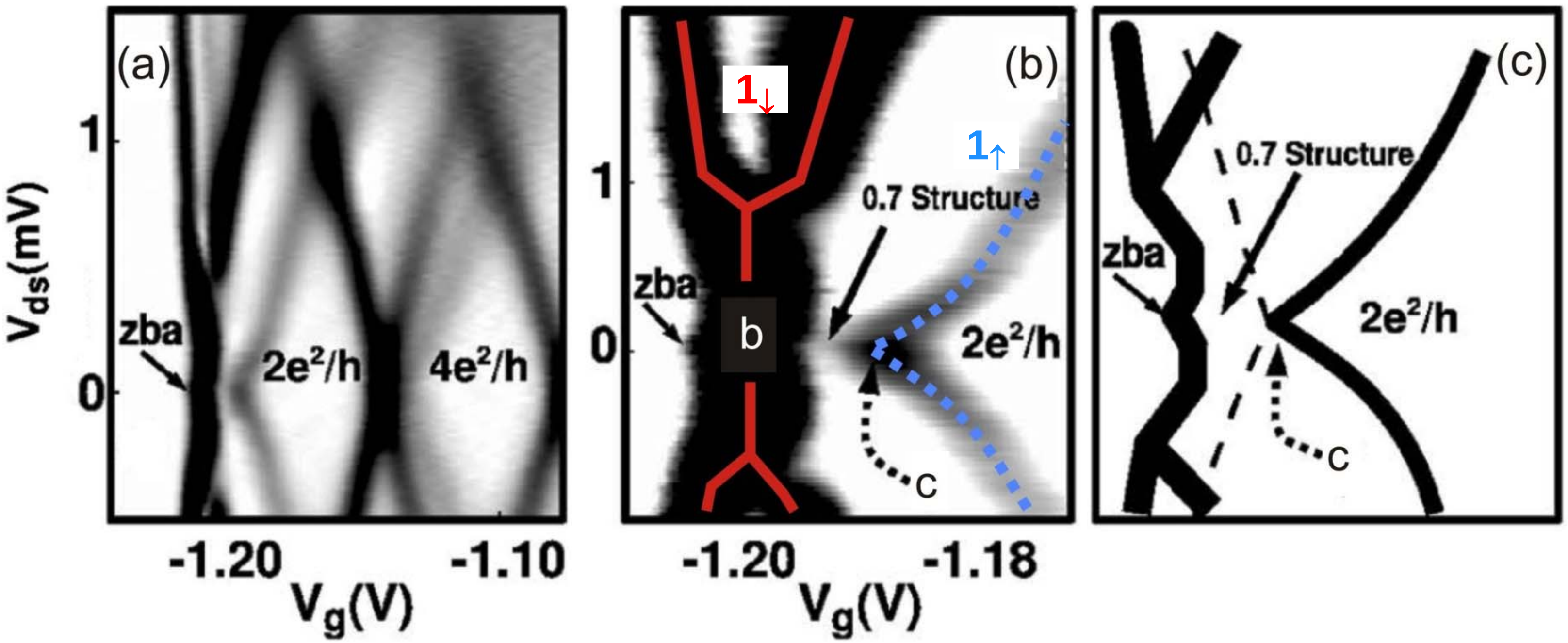

A.C. Graham *et al.*, PRB 75, 035331 (2007).

Teasing out what the subbands do at 0.7

- **These structures are common across a wide range of works…**

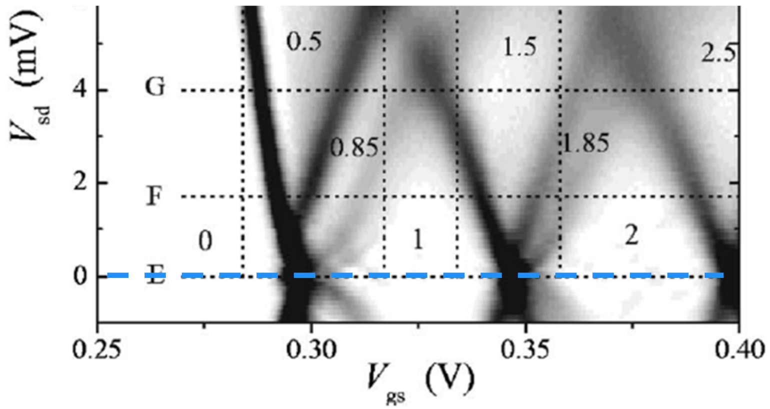

A. Kristensen *et al.*, PRB 62, 10950 (2000).

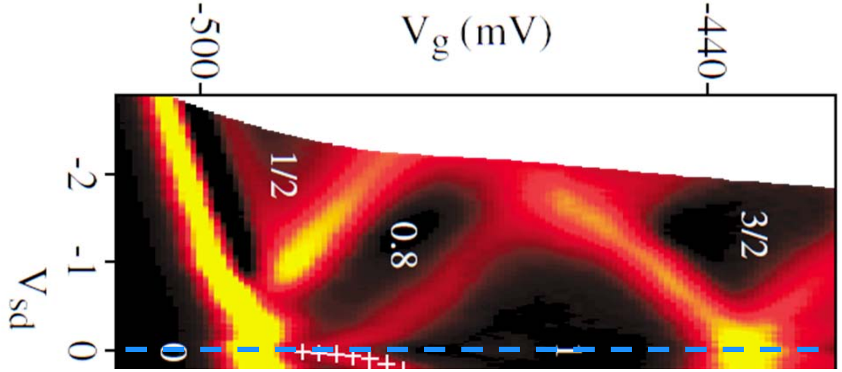

S.M. Cronenwett *et al.*, PRL 88, 226805 (2002).

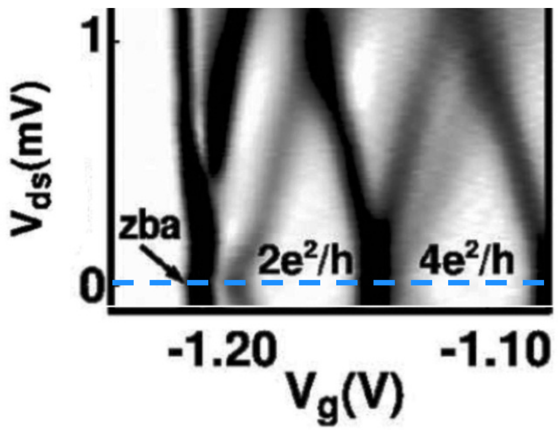

A.C. Graham *et al.*, PRB 75, 035331 (2007).

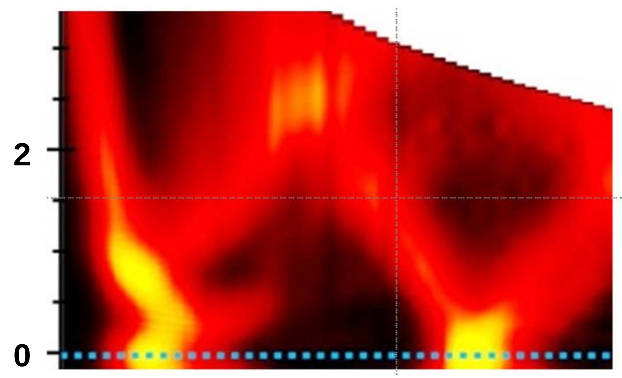

A.M. Burke *et al.*, Nano Lett. *in press*.

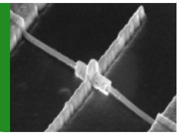

Moving beyond phenomenological models…

- **Lassl *et al.* performed calculations for a QPC using a non-equilibrium Green's function approach with the screened Coulomb interaction between electrons approximated as a repulsive contact potential:**

$$V_{\mathrm{int}}(\vec{r},\vec{r}\,') = \gamma\delta(\vec{r}-\vec{r}\,')$$

where $\gamma \cong 2\pi \times \hbar^2/(2m)$ is the interaction strength (but used as a variable).

- **A Keldysh Green-function approach is then used with a Hamiltonian operator $H^\sigma = H^\sigma_0 + \Sigma^\sigma_{\mathrm{int}}(\underline{r})$, where:**

$$H_0^\sigma = \frac{p_x^2+p_y^2}{2m} + V_{\mathrm{conf}}(x,y) + g\mu_B B\sigma$$

and:

$$\Sigma^\sigma_{\mathrm{int}}(\vec{r}) = \Sigma^\sigma_H + \Sigma^\sigma_F = \gamma n_{-\sigma}(\vec{r})$$

with:

$$n_\sigma(\vec{r}) = -\frac{i}{2\pi}\int dE\, G^<_\sigma(\vec{r},\vec{r},E)$$

A. Lassl *et al.*, PRB <u>75</u>, 045346 (2007).

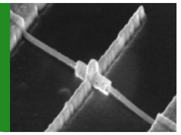

Moving beyond phenomenological models…

- **The problem is then discretized using the lattice below:**

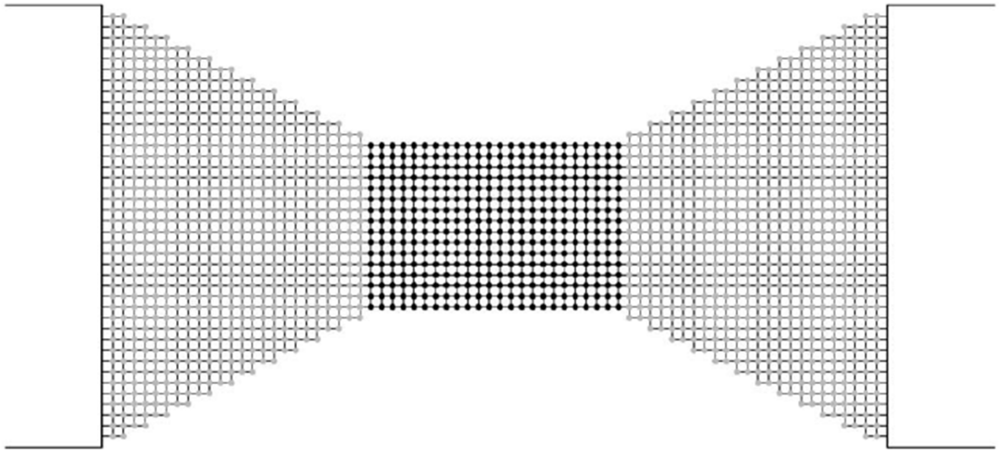

using a matrix approach with on-diagonal terms:

$$\mathcal{H}_{ii}^{\sigma} = 4\hbar^2/(2ma^2) + V_{\mathrm{conf}}(\vec{r}_i) + \Sigma_{\mathrm{int}}(\vec{r}_i) + g\mu_B B\sigma$$

where *a* is the lattice constant, neighbouring off-diagonal terms:

$$\mathcal{H}_{ij} = -\hbar^2/(2ma^2)$$

and all other off-diagonal terms as zero.

A. Lassl *et al.*, PRB 75, 045346 (2007).

Moving beyond phenomenological models…

- **The energy $E_1 = \hbar^2\pi^2/(2mW^2)$ where W is the width of the channel, with a small Zeeman field $E_z = 0.0015E_1$ added to break spin-symmetry.**

The $1_\uparrow$ subband pins just underneath μ before finally dropping to rejoin $1_\downarrow$, closing the spin-gap.

The energies of both $1_\uparrow$ and $1_\downarrow$ rises as the subband populates.

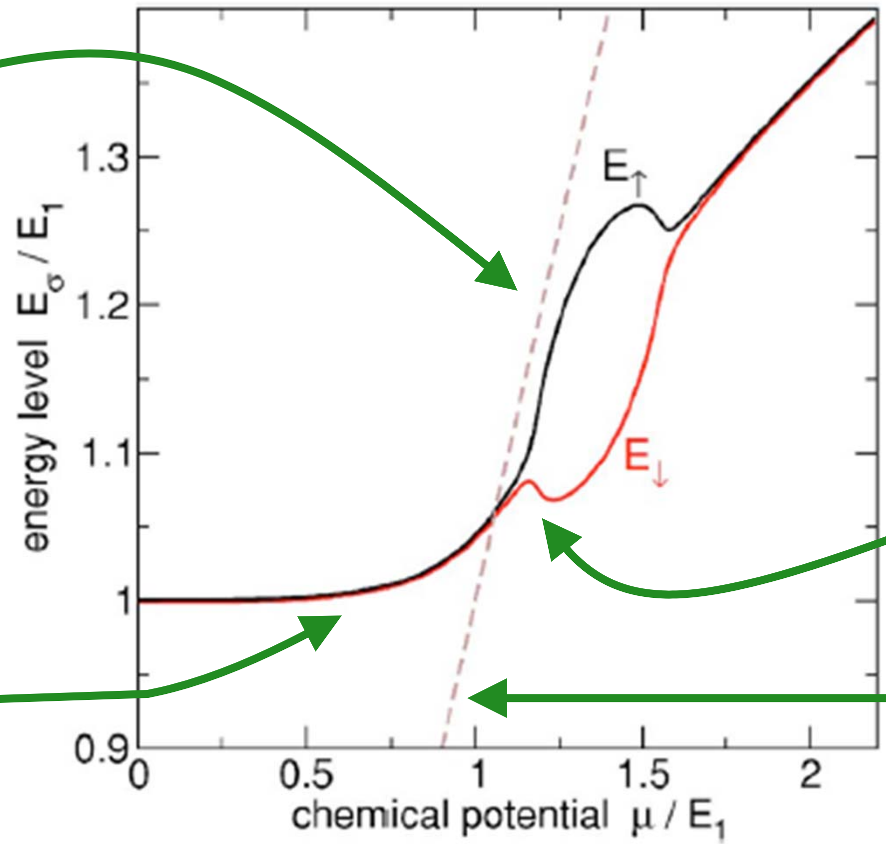

The $1_\downarrow$ subband rapidly drops in energy upon populating

The dashed line is the chemical potential μ

A. Lassl *et al.*, PRB 75, 045346 (2007).

Moving beyond phenomenological models…

- **The model does a great job of reproducing the experimental data, just as the Reilly model does:**

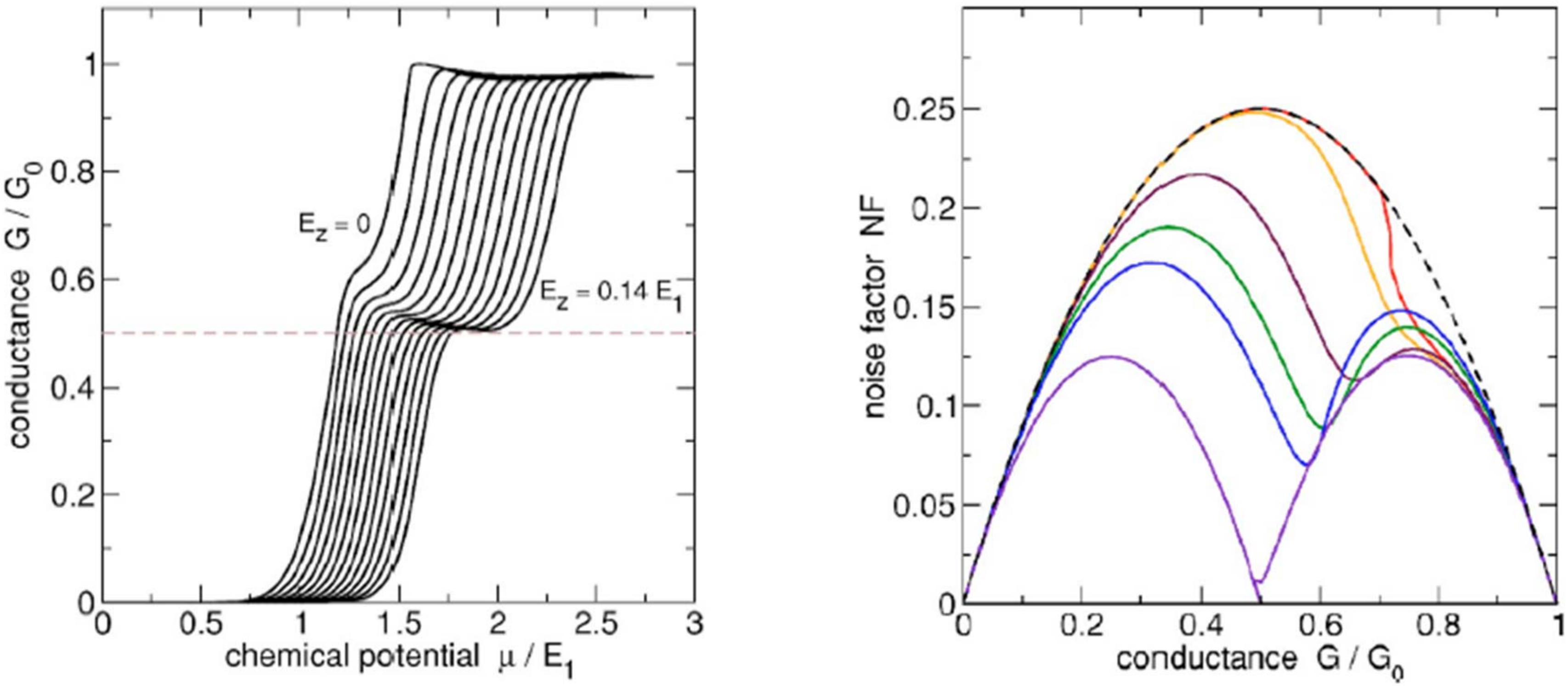

A. Lassl *et al.,* PRB 75, 045346 (2007).